


# Stable non-BPS black holes and black strings in five dimensions

Anshul Mishra<sup>\*</sup> and Prasanta K. Tripathy<sup>†</sup>

*Centre for Strings, Gravitation and Cosmology, Department of Physics,  
Indian Institute of Technology Madras, Chennai 600 036, India*

 (Received 27 October 2023; accepted 8 December 2023; published 2 January 2024)

In this paper we study black hole and black string solutions in five dimensional  $N = 2$  supergravity theories arising from the compactification of M-theory on Calabi-Yau manifolds. In particular, we consider explicit examples of three parameter Calabi-Yau manifolds which are obtained as hypersurfaces in toric varieties. Using the attractor mechanism, we obtain Bogomol'nyi-Prasad-Sommerfield (BPS) as well as non-BPS black holes in these compactified supergravity theories. We also consider the black string solutions in these models. We analyze the stability of these extremal black brane configurations by computing the recombination factor. We find multiple stable non-BPS attractor solutions in some of these models.

DOI: [10.1103/PhysRevD.109.026001](https://doi.org/10.1103/PhysRevD.109.026001)

## I. INTRODUCTION

It is well known that the compactification of string theory gives rise to a landscape of consistent low energy effective theories in various dimensions [1]. This landscape has further been enriched by the swampland program [2,3] which contrived a set of general criteria that the low energy effective theories must hold. One of the key ingredients devised in order to distinguish the low energy effective theories among each other is the weak gravity conjecture [4]. This conjecture tells that gravity is the weakest force among all and as a consequence objects with large charge must decay into their respective elementary constituents unless they are protected by a symmetry.

In gravity theories, black holes provide simplest objects which can be used to further analyze the weak gravity conjecture. Of particular interest are black hole configurations in  $N = 2$  supergravity theories. For these theories, the attractor mechanism [5–9] provides a suitable technique to construct the extremal black hole solutions. These extremal black holes may or may not preserve supersymmetry [8,9]. The attractor mechanism ensures that the scalar fields in these theories, which in general may take arbitrary values at spatial infinity, must run into fixed points at the horizon of the corresponding extremal black hole. Their values at the horizon are completely determined in terms of the black

hole charges. The attractor points in the moduli space correspond to critical points of a suitably constructed black hole effective potential [8]. This in turn determines the mass as well as entropy of these black holes.

Recently Long, Sheshmani, Vafa and Yau have constructed a number of non-Bogomol'nyi-Prasad-Sommerfield (BPS) black branes using the attractor mechanism [10]. They have considered  $N = 2$  supergravity theories in five dimensions [11], obtained upon the compactification of M-theory on Calabi-Yau manifolds [12,13].  $M2$  branes wrapped on two cycles of the Calabi-Yau manifold give rise to black holes and  $M5$  branes wrapped on four cycles give rise to black string configurations. Depending upon whether the two cycle corresponds to a holomorphic or a nonholomorphic curve one obtains a BPS or a non-BPS black hole. Likewise, if the four cycle is a (non)holomorphic divisor one obtains a (non)-BPS black string.

BPS objects, being protected by supersymmetry remain stable. Whereas the same thing may not hold for non-BPS configurations and a separate study is needed to address the issues of their stability. For non-BPS black holes, the attractor mechanism determines the black hole entropy. This, in turn is conjectured [10] to give rise to the asymptotic volume of the nonholomorphic curve on which the  $M2$  brane is wrapped provided the non-BPS black hole is doubly extremal. Similarly, for doubly extremal non-BPS black strings, the string tension determines the asymptotic volume of the nonholomorphic divisor on which the corresponding  $M4$  brane is wrapped. These nonholomorphic cycles correspond to local volume minimizers in a given homology class. If, within the same homology class there exists a piece-wise calibrated representative with a smaller volume then the black brane decays into the constituent brane/anti-brane pairs wrapping this piece-wise

<sup>\*</sup>anshulmishra2025@gmail.com

<sup>†</sup>prasanta@iitm.ac.in

*Published by the American Physical Society under the terms of the Creative Commons Attribution 4.0 International license. Further distribution of this work must maintain attribution to the author(s) and the published article's title, journal citation, and DOI. Funded by SCOAP<sup>3</sup>.*

representative cycle in accordance of the weak gravity conjecture. On the other hand, if no such piece-wise calibrated representative with a smaller volume exists within the same homology class then the black brane becomes stable against decay into constituent brane-anti-brane configurations. In the later case, the constituent brane configurations are said to be undergoing a recombination in order to form a stable non-BPS black brane [10]. Several examples of Calabi-Yau manifolds has been considered and it has been observed that the non-BPS black holes are always unstable [10]. On the other hand, it has been observed that some of these models admit stable non-BPS black strings [10].

These results have further been extended in [14] to consider an exhaustive study of all the two parameter Calabi-Yau compactifications of M-theory. It has been observed that the resulting non-BPS black hole configurations in all these examples are unstable and decay into the constituent BPS/non-BPS pairs. Moreover, for a given charge configuration, there exists a unique non-BPS black hole attractor. In contrast, there exist several non-BPS black string configurations which are stable against decay into constituent BPS/non-BPS pairs. In addition, many of these models also admit multiple basin of non-BPS black string attractors for a given charge configuration. Similar phenomena have also been observed in [15], in the context of four dimensional  $N = 2$  supergravity theories arising from the Calabi-Yau compactifications of type-*IIA* string theory. The authors have considered non-BPS  $D0 - D4$  as well as  $D0 - D2 - D4$  black hole configurations in one and two parameter Calabi-Yau models and made similar analysis. While many of these configurations are unstable, there are also examples of several stable non-BPS black holes in these classes of compactifications.

The authors in [10] considered a few examples of Calabi-Yau models with small  $h_{1,1}$  and interestingly the non-BPS black holes obtained in all their examples remained unstable. Surprisingly, this result holds true in all the two parameter examples considered in [14]. It remains to be seen whether this result holds for all five dimensional non-BPS black holes resulting in Calabi-Yau compactifications of M-theory. Further, the analysis of [14] shows the existence of multiple basin of attractors in some of these two-parameter models [16]. In models with larger  $h_{1,1}$  there is a possibility of obtaining more interesting black hole and black string configurations. In the present work we wish to generalize these results for a number of three parameter Calabi-Yau manifolds obtained as hypersurfaces in toric varieties. The cohomology data for these manifolds have been computed. Using these data we can obtain the black brane configurations and study their properties. In this paper we consider some of these three parameter models to obtain extremal black branes in them and analyze their properties.

The plan of the paper is as follows. First we will review the basic results on extremal black hole and black string

attractors in five-dimensional minimal supergravity in Sec. II. Also in this section we will set up our notations and conventions and outline the attractor equations that needs to be analyzed further. In Sec. III, we will shift our focus toward three parameter Calabi-Yau manifolds where we will outline some useful formulas and introduce some notations that will be used throughout the paper. Following a comprehensive treatment of BPS black holes in Sec. IV we turn our attention in particular to the black hole solutions resulting from the Calabi-Yau manifolds emerging as hypersurfaces in toric varieties (THCY). Subsequently, our investigation extends to non-BPS black hole solutions in Sec. V. In Sec. VA we take different examples of three parameter THCY models and investigate non-BPS black hole configurations. We also show the existence of multiple non-BPS black hole solutions. In Sec. VB we compute the recombination factor for non-BPS extremal black hole attractors in these THCY models and show that there exists stable non-BPS black holes. Moving forward, in Sec. VI we outline the essential details concerning extremal black string attractors in five-dimensional, minimal supergravity. Once again, we turn our attention into three-parameter Calabi-Yau manifolds. We take different cases for non-BPS black strings and obtain multiple solutions. We compute the recombination factor corresponding to these non-BPS extremal black strings in Sec. VIA highlighting the stability of these solutions. Finally we summarize our findings in Sec. VII.

## II. REVIEW OF 5D BLACK HOLE ATTRACTOR

In this section we will review the basics of black brane attractors in  $N = 2$  supergravity theory in five dimensions. We consider the five dimensional low energy effective theory arising upon the compactification of M-theory on a Calabi-Yau manifold. The corresponding Lagrangian density is given by [17]

$$\begin{aligned} \frac{\mathcal{L}}{\sqrt{-\mathbf{g}}} = & -\frac{1}{2}R - \frac{1}{4}G_{IJ}F_{\mu\nu}^I F^{J\mu\nu} - \frac{1}{2}g_{ij}\partial_\mu\phi^i\partial^\mu\phi^j \\ & + \frac{1}{6^{3/2}\sqrt{-\mathbf{g}}}C_{IJK}\epsilon^{\lambda\mu\nu\rho\sigma}F_{\lambda\mu}^I F_{\nu\rho}^J A_\sigma^K. \end{aligned} \quad (2.1)$$

Here  $\mathbf{g}_{\mu\nu}$  is the space-time metric and  $\mathbf{g}$  is its determinant.  $R$  is the corresponding Ricci scalar,  $\phi^i$  are the real scalar fields arising from the Kähler moduli  $t^I (I = 1, \dots, h_{1,1})$ , and  $A_\mu^I$  are the gauge fields in the vector multiplet with corresponding field strengths  $F_{\mu\nu}^I$ . The triple intersection numbers of the Calabi-Yau manifold are denoted by  $C_{IJK}$ . The volume of the Calabi-Yau manifold is constrained to satisfy

$$C_{IJK}t^I t^J t^K = 1. \quad (2.2)$$

Thus, only  $h_{1,1} - 1$  real scalar fields are independent and are denoted by  $\phi^i$ . The moduli space metric  $g_{ij}$  is given by

$$g_{ij} = \frac{3}{2} \partial_i t^l \partial_j t^l G_{IJ}, \quad g^{ij} g_{jk} = \delta_k^i, \quad (2.3)$$

Here  $G_{IJ}$  is the pull back of moduli space metric onto the ‘‘ambient space’’ formed by the Kähler moduli  $t^l$ . The metric  $G_{IJ}$  is derived from the prepotential  $\mathcal{V} = C_{IJK} t^I t^J t^K$  as

$$G_{IJ} := -\frac{1}{3} \frac{\partial^2 \log C_{LMN} t^L t^M t^N}{\partial t^I \partial t^J} \Big|_* \\ = (3C_{ILM} C_{JNP} t^L t^M t^N t^P - 2C_{IJM} t^M) \Big|_*, \quad (2.4)$$

where ‘‘\*’’ indicates that we need to impose the constraint (2.2) after taking the derivatives.

The critical points of this theory have been studied extensively in [18] using the attractor mechanism. The model admits extremal black hole as well as extremal black string solutions. We will first review the black hole configurations. These are electrically charged objects carrying charges  $q_I$ . They are described in terms the black hole effective potential [18]

$$V = G^{IJ} q_I q_J = Z^2 + \frac{3}{2} g^{ij} \partial_i Z \partial_j Z. \quad (2.5)$$

Here  $Z$  denotes the central charge of the black hole  $Z = q_I t^I$ . The critical points of this potential are given by

$$\partial_i V = 0. \quad (2.6)$$

For a comprehensive treatment of the critical points using the so called new attractor approach see [19,20]. The above condition is obviously satisfied by the extrema of the central charge  $Z$ . All such critical points correspond to supersymmetry preserving extremal black holes. However, there exist critical points which do not extremize  $Z$ . These correspond to nonsupersymmetric extremal black holes. For both these cases, the entropy of the black hole is determined by the value  $V_0$  of the effective potential (2.5) at the critical point. In the present convention, the black hole entropy is given by

$$S = 2\pi \left( \frac{V_0}{9} \right)^{3/4}. \quad (2.7)$$

To obtain the equation of motion it is more convenient to express the black hole effective potential as [14]

$$V = \frac{3}{2} Z^2 - \frac{1}{2} C^{IJ} q_I q_J. \quad (2.8)$$

Here we have introduced the notation  $C_{IJ} = C_{IJK} t^K$  and  $C^{IJ}$  is the matrix inverse of  $C_{IJ}$ . Upon extremizing the potential (2.8) with the constraint (2.2), we obtain

$$3Z(q_K - ZC_{KIJ} t^I t^J) + \frac{1}{2} (C^{IL} C^{JM} C_{KLM} \\ - C^{IJ} C_{KLM} t^L t^M) q_I q_J = 0. \quad (2.9)$$

The supersymmetric critical points  $\partial_i Z = 0$  are given by

$$q_K - ZC_{KIJ} t^I t^J = 0. \quad (2.10)$$

Clearly, the first term of (2.9) vanishes if the above is satisfied. With a little bit of work it can be shown that the second term of this equation also vanishes for the supersymmetric critical points. The equation of motion (2.9) also admits critical points for which (2.10) does not hold. These correspond to non-BPS critical points of the effective potential (2.8). To find these non-BPS critical points, we set

$$X_I := q_I - ZC_{IJK} t^J t^K \quad (2.11)$$

Using this notation, we will rewrite (2.9) in a suitable form [14]. To this end, substitute  $q_I = X_I + ZC_{IJK} t^J t^K$  in (2.9) to obtain

$$8ZX_K + C_{KLM} (C^{IL} C^{JM} - C^{IJ} t^L t^M) X_I X_J = 0. \quad (2.12)$$

Clearly,  $X_I = 0$  solves this equation trivially and gives BPS critical points. Solutions of (2.12) with  $X_I \neq 0$  correspond to non-BPS critical points.

To further analyze the above equation, we note that the constraint (2.2) can be rewritten in terms of  $X_I$  as

$$t^I X_I = 0. \quad (2.13)$$

We can first solve the above constraint to express  $X_I$  in terms of  $t^I$  and substitute the resulting values in (2.12) which can then be solved to obtain the critical points. Care must be taken while solving (2.13) for  $X_I$ , since it remains unchanged upon multiplying the  $X_I$ s by an overall factor. The overall multiplicative factor in the  $X_I$ s can be determined as follows. Multiply both sides of (2.12) with  $C^{KN} X_N$  and using (2.13) to obtain

$$8ZC^{IJ} X_I X_J + C_{KLM} C^{KI} C^{LJ} C^{MN} X_I X_J X_N = 0. \quad (2.14)$$

This equation is not homogeneous in  $X_I$  and hence will fix the overall multiplicative factor in it uniquely. Using the above formalism, models with  $h_{1,1} = 2$  have been extensively analyzed in [14]. In the following we will consider some explicit examples of Calabi-Yau compactifications with  $h_{1,1} = 3$  and analyze the resulting black hole solutions.

Before we turn our discussion on three parameter Calabi-Yau models, we will outline the Kähler cone condition, which states that the volume of any effective curve must be positive:

$$\int_C J > 0, \quad (2.15)$$

where  $J = t^I J_I$  is the Kähler form and  $C$  is any arbitrary effective curve in the Calabi-Yau manifold  $\mathcal{M}$ . Here  $\{J_I\}$  form an integral basis of the cohomology class  $H_{1,1}(\mathcal{M}, \mathbb{Z})$ . Thus, as emphasized in [10], we need to make sure that the resulting solutions for the attractors must lie within the Kähler cone.

### III. THREE PARAMETER MODEL

Our goal in the present work is to analyze black brane attractors in three parameter Calabi-Yau models. In this section we will set up some notations in three parameter models that will be used throughout this paper to analyze the equations of motion. First, for convenience introduce the variables  $x, y, z$  to represent the Kähler moduli  $t^1, t^2, t^3$  respectively. Further, introduce the parameters  $a, b, \dots$ , to denote the intersection numbers  $C_{IJK}$  such that  $C_{111} = a, C_{112} = b, C_{122} = c, C_{222} = d, C_{113} = e, C_{123} = f, C_{133} = g, C_{223} = h, C_{233} = i, C_{333} = j$ . In addition, we introduce the functions  $A_1, \dots, A_6$  as

$$\begin{aligned} A_1 &= ax + by + ez, & A_2 &= bx + cy + fz, \\ A_3 &= ex + fy + gz, & A_4 &= cx + dy + hz, \\ A_5 &= fx + hy + iz, & A_6 &= gx + iy + jz. \end{aligned} \quad (3.1)$$

With these notations, the matrix  $C_{IJ} = C_{IJK} t^K$  reads as

$$C_{IJ} = \begin{pmatrix} A_1 & A_2 & A_3 \\ A_2 & A_4 & A_5 \\ A_3 & A_5 & A_6 \end{pmatrix}. \quad (3.2)$$

To express the inverse of the matrix  $C_{IJ}$  in an organized way we introduce the functions  $B_1, \dots, B_6$  as and

$$\begin{aligned} B_1 &= A_4 A_6 - A_5^2, & B_2 &= A_3 A_5 - A_2 A_6, \\ B_3 &= A_2 A_5 - A_3 A_4, & B_4 &= A_1 A_6 - A_3^2, \\ B_5 &= A_2 A_3 - A_1 A_5, & B_6 &= A_1 A_4 - A_2^2. \end{aligned} \quad (3.3)$$

In terms of these quantities, the matrix inverse  $C^{IJ}$  is expressed as

$$C^{IJ} = \frac{1}{A_1 B_1 + A_2 B_2 + A_3 B_3} \begin{pmatrix} B_1 & B_2 & B_3 \\ B_2 & B_4 & B_5 \\ B_3 & B_5 & B_6 \end{pmatrix}. \quad (3.4)$$

We further need the expressions for quantities such as  $C_I \equiv C_{IJK} t^J t^K$  and  $C^{IJ} q_J$ . It is straightforward to obtain

$$C_I = C_{IJK} t^J t^K = \begin{pmatrix} A_1 x + A_2 y + A_3 z \\ A_2 x + A_4 y + A_5 z \\ A_3 x + A_5 y + A_6 z \end{pmatrix}, \quad (3.5)$$

and

$$C^{IJ} q_J = \frac{1}{A_1 B_1 + A_2 B_2 + A_3 B_3} \begin{pmatrix} B_1 q_1 + B_2 q_2 + B_3 q_3 \\ B_2 q_1 + B_4 q_2 + B_5 q_3 \\ B_3 q_1 + B_5 q_2 + B_6 q_3 \end{pmatrix}. \quad (3.6)$$

The central charge  $Z = q_I t^I$  is given as

$$Z = (q_1 x + q_2 y + q_3 z), \quad (3.7)$$

and the black hole effective potential (2.8) becomes

$$V = \frac{3}{2} (q_1 x + q_2 y + q_3 z)^2 \frac{(B_1 q_1^2 + 2B_2 q_1 q_2 + 2B_3 q_1 q_3 + 2B_5 q_2 q_3 + B_4 q_2^2 + B_6 q_3^2)}{2(A_1 B_1 + A_2 B_2 + A_3 B_3)}. \quad (3.8)$$

### IV. BPS BLACK HOLES

We will first analyze the BPS black holes in three parameter Calabi-Yau models. Thus, we need to solve the Eq. (2.10) subjected to the constraint (2.2). For the three parameter models, (2.10) becomes

$$\begin{aligned} Z(A_1 x + A_2 y + A_3 z) &= q_1, \\ Z(A_2 x + A_4 y + A_5 z) &= q_2, \\ Z(A_3 x + A_5 y + A_6 z) &= q_3. \end{aligned} \quad (4.1)$$

On the other hand the constraint (2.2) becomes

$$\begin{aligned} x(A_1 x + A_2 y + A_3 z) + y(A_2 x + A_4 y + A_5 z) \\ + z(A_3 x + A_5 y + A_6 z) = 1. \end{aligned} \quad (4.2)$$

To further analyze the above conditions, note that the left hand sides in Eqs. (4.1) and (4.2) are all degree three homogeneous polynomials in  $x, y, z$ . We will introduce the following inhomogeneous coordinates  $\tau = x/z$  and  $t = y/z$ . Further we define the charge ratios  $\rho = q_1/q_3$

and  $\sigma = q_2/q_3$ . In terms of these variables, Eqs. (4.1) becomes

$$z^3(\rho\tau + \sigma t + 1)(a\tau^2 + 2b\tau t + ct^2 + 2e\tau + 2ft + g) = \rho, \quad (4.3)$$

$$z^3(\rho\tau + \sigma t + 1)(b\tau^2 + 2c\tau t + dt^2 + 2f\tau + 2ht + i) = \sigma, \quad (4.4)$$

$$z^3(\rho\tau + \sigma t + 1)(e\tau^2 + 2f\tau t + 2g\tau + ht^2 + 2it + j) = 1. \quad (4.5)$$

The constraint on the volume becomes

$$z^3(a\tau^3 + 3b\tau^2t + 3c\tau t^2 + dt^3 + 3e\tau^2 + 6f\tau t + 3g\tau + 3ht^2 + 3it + j) = 1 \quad (4.6)$$

Using the above equation, we can eliminate  $z$  in Eqs. (4.3)–(4.5). This results in three equations in two variables. However, as we will see below, only two of them remain independent. We need to solve two of these equations for  $\tau$  and  $t$  in terms of the charge ratios  $\rho$  and  $\sigma$ . However, notice that these equations provide two coupled cubics in two variables. Thus, it is not possible to obtain an exact analytic solution for arbitrary values of the intersection numbers. In order to obtain some insight into the problem we will first study the inverse problem, i.e., we will solve these equations for the charge ratios  $\rho$  and  $\sigma$  in terms of the scalar moduli  $\tau$  and  $t$ . Since these equations are linear in  $\rho$  and  $\sigma$ , it is straightforward to obtain the solution. Consider the first to Eqs. (4.3) and (4.4). We find

$$\begin{aligned} \rho &= \frac{a\tau^2 + 2b\tau t + ct^2 + 2e\tau + 2ft + g}{e\tau^2 + 2f\tau t + 2g\tau + ht^2 + 2it + j}, \\ \sigma &= \frac{b\tau^2 + 2c\tau t + dt^2 + 2f\tau + 2ht + i}{e\tau^2 + 2f\tau t + 2g\tau + ht^2 + 2it + j}. \end{aligned} \quad (4.7)$$

It can easily be verified that (4.5) holds true upon substitution of the above values for  $\rho$  and  $\sigma$  in it.

In this paper we will consider some specific examples of three parameter Calabi-Yau manifolds. We will consider Calabi-Yau manifolds which are obtained as hypersurfaces from toric varieties. A toric variety is given in terms of a reflexive polytope with a specific triangulation of its faces. A polytope is reflexive provides it is integral (i.e., the coordinates of its vertices are all integers) and the corresponding dual polytope is also integral. The faces of a reflexive polytope are in one to one correspondence with the vertices of the dual polytope. Consider a reflexive polytope with  $n$  faces and let the  $n$  vectors  $\vec{v}_i$ , ( $i = 1, \dots, n$ ) represent the vertices of the dual polytope. In general, they will not all be linearly independent, and, for a polytope in  $d$  dimensions, we will have  $(n - d)$  relations like

$$\sum_{i=1}^n q_i^r \vec{v}_i = 0. \quad (4.8)$$

Here the index  $r$  takes values  $r = 1, \dots, n - d$ . We associate each of the vertices with a homogeneous coordinate  $z_i \in \mathbb{C}^n$ . If we view the coefficients  $q_i^r$  in (4.8) as elements of a  $(n - d) \times n$  weight matrix, then each of its row defines an equivalence relation among these  $n$  homogeneous coordinates with the corresponding coefficients as the weights. Thus there are  $(n - d)$  such equivalence relations altogether. Removing the fixed points and taking quotient with these equivalence relations we obtain a  $d$  dimensional toric variety. A hypersurface of vanishing first Chern class in this toric variety gives a  $(d - 1)$  dimensional Calabi-Yau manifold.

We are interested in Calabi-Yau threefolds. Thus we need to construct toric varieties from four dimensional reflexive polytopes. All such reflexive polytopes in four dimensions have been classified by Kreuzer and Sakrke [21]. The cohomology data for the corresponding toric Calabi-Yau manifolds have been computed in [22–24] and the results are listed in the database [25]. In the present work, we will use the cohomology data such as the intersection numbers and Kähler cone conditions from [25] to analyze the black brane configurations.

We will now consider an explicit example of a toric hypersurface Calabi-Yau manifold (THCY). The polytope ID associated with this THCY as per the Kreuzer-Sakrke classification [21] is 260. In the following we will recapitulate some of the essential cohomology data associated with it from the Calabi-Yau database [25]. The Hodge numbers for the Calabi-Yau manifold  $\mathcal{M}$  are  $h_{1,1} = 3$  and  $h_{2,1} = 123$  and the corresponding Euler number is  $-260$ . The resolved weight matrix of  $\mathcal{M}$  has the form

$$Q = \begin{pmatrix} 0 & 0 & 0 & 1 & 1 & 3 & 1 \\ 0 & 1 & 1 & 2 & 2 & 6 & 0 \\ 1 & 0 & 0 & 0 & 1 & 2 & 0 \end{pmatrix}. \quad (4.9)$$

The volume of the manifold is given by

$$\mathcal{V} = 2xy^2 + 2xyz + 4y^3 - 4yz^2. \quad (4.10)$$

From this we can obtain the intersection numbers of the Calabi-Yau manifold  $\mathcal{M}$ . We find the nonvanishing intersection numbers to be  $c = 2/3, d = 4, f = 1/3, i = -4/3$ .

Each of the homogeneous coordinates  $z_i$  associated with the toric Calabi-Yau  $\mathcal{M}$  define a holomorphic divisor  $D_i$ . Denoting the basis elements of  $(1,1)$  homology class of  $\mathcal{M}$  as  $\{J_1, J_2, J_3\}$ , the divisor classes  $D_i$  in terms of them are given as  $D_1 = -2J_1 + J_2 - J_3, D_2 = J_1, D_3 = J_1, D_4 = 2J_1 + J_3, D_5 = J_2, D_6 = 2J_1 + 2J_2 + J_3, D_7 = J_3$ .

The Mori cone matrix associated with  $\mathcal{M}$  is

$$\mathcal{M}^i_j = \int_{C^i} D_j = C^i \cdot D_j = \begin{pmatrix} 0 & 1 & 1 & 0 & 0 & 0 & -2 \\ 1 & 0 & 0 & 0 & 1 & 2 & 0 \\ -1 & 0 & 0 & 1 & 0 & 1 & 1 \end{pmatrix}. \quad (4.11)$$

The elements of the Mori cone matrix indicate the intersection of generating curves  $C^i (i = 1, \dots, 3)$  with the toric divisor classes  $D_i (i = 1, \dots, 7)$  [23]. In order to ensure the validity of the Kähler cone condition (2.15) for our attractors, we also need the Kähler cone matrix  $K$  corresponding to the Calabi-Yau manifold. This is the matrix whose elements  $K^i_j$  are defined by [23]

$$K^i_j = \int_{C^i} J_j. \quad (4.12)$$

From the expression for the Mori cone matrix we can find the Kähler cone matrix. In the present case, the Kähler cone matrix is given by

$$K = \begin{pmatrix} 1 & 0 & -2 \\ 0 & 1 & 0 \\ 0 & 0 & 1 \end{pmatrix}. \quad (4.13)$$

This indicates that the Kähler moduli  $t^I$  for this model will lie inside the Kähler cone provided  $x - 2z > 0$ ,  $y > 0$ ,  $z > 0$ . In terms of the inhomogeneous coordinates these conditions become  $\tau - 2 > 0$ ,  $t > 0$  and  $z > 0$ . Now, consider the constraint on the volume (2.2) in terms of the inhomogeneous coordinates:

$$2z^3 t(t+1)(\tau+2t-2) = 1. \quad (4.14)$$

From the above constraint we observe that  $z$  becomes positive in the region  $t > 0$ ,  $\tau > 2$ . Thus, we do not need to impose it as an additional condition for the solution to remain inside the Kähler cone.

We will now consider the BPS solutions for this model. Substituting the values of the intersection numbers in (4.7) we can obtain the charge ratios in terms of the inhomogeneous coordinates. However, in this case the BPS equations  $q_I - Z C_{IJK} t^J t^K = 0$  are simple enough to solve directly. Substituting the values of the intersection numbers and rescaling the charges and variables appropriately, the equations take the form

$$\begin{aligned} 3\rho - 2t(t+1)z^3(\rho\tau + \sigma t + 1) &= 0, \\ 3\sigma - 2z^3(6t^2 + 2\tau t + \tau - 2)(\rho\tau + \sigma t + 1) &= 0. \end{aligned} \quad (4.15)$$

The variable  $z$  in the above equations can be eliminated using the constraint (4.14) to obtain

$$\begin{aligned} \frac{2\rho(3t + \tau - 3) - \sigma t - 1}{\tau + 2t - 2} &= 0, \\ \sigma - \frac{(6t^2 + 2\tau t + \tau - 2)(\rho\tau + \sigma t + 1)}{3t(t+1)(\tau + 2t - 2)} &= 0. \end{aligned} \quad (4.16)$$

These equations can easily be solved to obtain a unique solution for  $\tau$  and  $t$  in terms of the charge ratios  $\rho$  and  $\sigma$ :

$$\tau = \frac{24\rho^2 - 4\rho(\sigma - 3) - \sigma + 1}{\rho(6\rho - \sigma + 2)}, \quad t = -\frac{2\rho + 1}{6\rho - \sigma + 2}. \quad (4.17)$$

The entropy associated with the attractor is

$$S = \frac{2\pi}{3\sqrt{3}} |Z|^{3/2} \quad (4.18)$$

Upon substituting the solution (4.17) in the above and simplifying we find

$$S = 2^{1/3} \sqrt{3} \pi q_3^2 (\rho(2\rho + 1)(4\rho - \sigma + 1))^{2/3}. \quad (4.19)$$

We need to make sure that the solution (4.17) lies within the Kähler cone, i.e., we must have  $\tau > 2$  and  $t > 0$ . Expressed in terms of the charge ratios, these conditions become

$$\frac{(2\rho + 1)(6\rho - \sigma + 1)}{\rho(6\rho - \sigma + 2)} > 0 \quad \text{and} \quad \frac{2\rho + 1}{6\rho - \sigma + 2} < 0. \quad (4.20)$$

To simplify the above conditions further, note that for the attractor solution (4.17), we have  $\rho^2(\tau + 2t - 2) = \rho(2\rho + 1)(t + 1)$ . Since both  $(\tau + 2t - 2)$  and  $(t + 1)$  are positive inside the Kähler cone, we must have  $\rho(2\rho + 1) > 0$ . Thus, we can have  $\rho > 0$  or  $\rho < -1/2$ . Now, requiring  $\tau > 2$  gives the condition

$$\frac{6\rho - \sigma + 1}{6\rho - \sigma + 2} > 0. \quad (4.21)$$

Thus, for a given  $\rho$  we can either have  $6\rho - \sigma + 1 > 0$  or  $6\rho - \sigma + 2 < 0$ . In other words, for  $\tau > 2$  we must have  $\sigma > (6\rho + 2)$  or  $\sigma < (6\rho + 1)$ . We will now consider the implication of these two bounds on  $\sigma$  on the  $t > 0$  condition. Note that for  $\sigma > (6\rho + 2)$  we have  $(6\rho + 2 - \sigma) < 0$  and hence  $t > 0$  implies  $2\rho + 1 > 0$  and hence  $\rho$  must be positive. For  $\sigma < (6\rho + 1)$  we have  $(6\rho + 1 - \sigma) > 0$  and hence  $(6\rho + 2 - \sigma)$  is positive. Thus  $2\rho + 1 < 0$  and hence  $\rho < -1/2$ . To summarize, the solution (4.17) lies within the Kähler cone provided  $\rho > 0, \sigma > (6\rho + 2)$  or  $\rho < -1/2, \sigma < (6\rho + 1)$ .

Before we turn our attention to the non-BPS black holes, we will consider one more example of a three parameter THCY model. The polytope ID associated with this THCY is 230. It has Hodge numbers  $h_{1,1} = 3, h_{2,1} = 111$  and

Euler number  $\chi = -216$ . The resolved weight matrix associated with it is given by

$$Q = \begin{pmatrix} 0 & 0 & 0 & 0 & 0 & 1 & 1 \\ 0 & 1 & 1 & 1 & 1 & 3 & 0 \\ 1 & 1 & 1 & 0 & 0 & 3 & 0 \end{pmatrix}. \quad (4.22)$$

The volume of the Calabi-Yau manifold  $\mathcal{M}$  is given by

$$\mathcal{V} = 2x^3 + 2x^2y + x^2z - 3xz^2 + 9z^3 \quad (4.23)$$

From the above we can read the respective intersection numbers. We find  $a = 2, b = 2/3, e = 1/3, g = -1, j = 9$  and all other intersection numbers are zero. The Mori cone matrix associated with the manifold  $\mathcal{M}$  is

$$\mathcal{M}^i_j = \int_{C^i} D_j = \begin{pmatrix} -1 & 0 & 0 & 1 & 1 & 0 & 0 \\ 0 & 0 & 0 & 0 & 0 & 1 & 1 \\ 1 & 1 & 1 & 0 & 0 & 0 & -3 \end{pmatrix}, \quad (4.24)$$

where  $\{C^i\}$  are the Mori cone generators. The divisor classes  $D_j$  are given in terms of the basis  $\{J_1, J_2, J_3\}$  of  $(1,1)$  homology class as  $D_1 = J_1 - J_2, D_2 = J_1, D_3 = J_1, D_4 = J_2, D_5 = J_2, D_6 = 3J_1 - J_3, D_7 = J_3$ . From (4.24) we find the Kähler cone matrix  $K$  for  $\mathcal{M}$  to be

$$K = \begin{pmatrix} 0 & 1 & 0 \\ 0 & 0 & 1 \\ 1 & 0 & -3 \end{pmatrix}. \quad (4.25)$$

We can now study the BPS solutions for this model. Substituting the values of the intersection numbers in (4.7) it can be seen that the charge ratios in this case take the form

$$\sigma = \frac{2\tau^2}{\tau^2 - 6\tau + 27}, \quad \rho = \frac{6\tau^2 + (4t + 2)\tau - 3}{\tau^2 - 6\tau + 27}. \quad (4.26)$$

Now we have much a simpler expression and it can be inverted to find the inhomogeneous moduli  $\tau$  and  $t$  in terms of  $\sigma$  and  $\rho$ . We find

$$\begin{aligned} \tau &= \frac{3}{\sigma - 2} \left( \sigma \pm \sqrt{2(3\sigma - \sigma^2)} \right), \\ t &= \frac{\rho\tau^2 - 6\rho\tau + 27\rho - 6\tau^2 - 2\tau + 3}{4\tau}, \end{aligned} \quad (4.27)$$

for  $\sigma \neq 2$ . For  $\sigma = 2$ , we have

$$\tau = \frac{9}{2}, \quad t = \frac{1}{24}(27\rho - 170). \quad (4.28)$$

Upon substituting the solution in the expression for the entropy (4.18) and simplifying, we find

$$S = \frac{\pi}{12} \left( \frac{2q_3^3}{3\tau^3} \right)^{1/2} \frac{(\rho^2(\tau^2 - 6\tau + 27) - \rho(6\tau^2 + 2\tau - 3) + 4\tau(\sigma\tau + 1))^{3/2}}{(\rho\tau(\tau^2 - 6\tau + 27) - (2\tau^3 + 3\tau - 18))^{1/2}}. \quad (4.29)$$

Here for simplicity we have expressed the  $\sigma$  dependence through  $\tau$  as given in (4.27).

Several comments are in order. First, since  $\tau$  and  $t$  are real valued we must have  $3\sigma - \sigma^2 > 0$ , *i.e.*,  $\sigma$  lies in the range  $0 \leq \sigma \leq 3$ . Further, the values must lie within the Kähler cone. From the Kähler cone matrix (4.25), we find that  $y > 0, z > 0$  and  $x - 3z > 0$ . Thus, we have  $\tau > 3$  and  $t > 0$ . We also need to ensure that  $z$  remains positive for both the solutions. We can do so by examining the volume constraint (2.2), which in our model takes the form:

$$z^3(2\tau^3 + (2t + 1)\tau^2 - 3\tau + 9) = 1. \quad (4.30)$$

Notice that the quantity  $(2\tau^3 + (2t + 1)\tau^2 - 3\tau + 9)$  in the left hand side above remains positive for  $\tau > 3$  and  $t > 0$ . Thus, imposing the volume constraint (2.2),  $z$  becomes automatically positive provided  $\tau > 3$  and  $t > 0$ . We do not need to impose this condition separately for the solutions to lie inside the Kähler cone.

For  $\sigma = 2$ , from (4.28) we find a unique solution lying within the Kähler cone provided  $\rho > 170/27$ . For  $\sigma \neq 2$  we have two possible solutions as given in (4.27). First consider the following solution for  $\tau$ :

$$\tau = \frac{3}{\sigma - 2} \left( \sigma + \sqrt{2\sigma(3 - \sigma)} \right). \quad (4.31)$$

It may be observed that, for  $0 \leq \sigma < 2$  the value of  $\tau$  becomes negative and hence lies outside the Kähler cone. On the other hand, for  $2 < \sigma \leq 3$  the value of  $\tau$  is always greater than 3 and hence lies within the Kähler cone. We can substitute this value of  $\tau$  in the expression for  $t$  in (4.26). We find that, for  $2 < \sigma \leq 3$  the value of  $t$  remains positive provided

$$\rho > \rho_- \equiv \frac{1}{54} \left( (169\sigma - 6) - 4\sqrt{2\sigma(3 - \sigma)} \right). \quad (4.32)$$

For  $\sigma = 2$ ,  $\rho_-$  takes the minimum possible value  $\rho_- = 6$ . Thus, this branch of BPS attractors exists for  $2 < \sigma \leq 3$  and  $\rho > 6$ .

We will now consider the second solution for  $\tau$  in (4.27):

$$\tau = \frac{3}{\sigma - 2} \left( \sigma - \sqrt{2\sigma(3 - \sigma)} \right). \quad (4.33)$$

It is easy to notice that, for  $1 < \sigma \leq 3$  the value of  $\tau$  remains greater than 3 and it lies within the Kähler cone. Substituting the above expression for  $\tau$  in the expression for  $t$  in (4.27) we find that it remains positive provided

$$\rho > \rho_+ \equiv \frac{1}{54} \left( (169\sigma - 6) + 4\sqrt{2\sigma(3 - \sigma)} \right). \quad (4.34)$$

Since  $\rho_+$  monotonically increases with  $\sigma$ , it takes the minimum possible value  $\rho_+ = 19/6$  at  $\sigma = 1$ . This branch exists for  $1 < \sigma \leq 3$  and  $\rho > 19/6$ .

From the above we can see that, while no solution exists for  $\sigma < 1$ , we have a unique solution described by (4.33) and the corresponding  $t$  when  $\rho > \rho_+$  and  $\sigma$  takes values in the range  $1 < \sigma \leq 2$ . On the other hand, for  $2 < \sigma < 3$  there is a possibility of existence of both the solutions. Notice that  $\rho_+ \geq \rho_-$ , with the equality holding for  $\sigma = 3$ . Thus, we have a unique solution described by (4.31) (and the corresponding solution for  $t$ ) if  $2 < \sigma \leq 3$  and  $\rho_- < \rho < \rho_+$ , whereas both the solutions exist if  $\rho > \rho_+$ .

As a concrete example, take  $\sigma = 3/2$  and  $\rho = 5$ . In this case the equations of motion gives rise to a unique solution inside the Kähler cone

$$\tau = 9(\sqrt{2} - 1), \quad t = \frac{1}{12}(19\sqrt{2} - 23),$$

and 
$$z = \left( \frac{2}{9(1887\sqrt{2} - 2641)} \right)^{1/3}. \quad (4.35)$$

Similarly, consider the values  $\sigma = 5/2$  and  $\rho = 38/5$ . We find

$$\tau = 3(5 + \sqrt{10}), \quad t = \frac{1}{300}(13\sqrt{10} - 35),$$

$$z = \left( \frac{30267}{2} + \frac{46773}{\sqrt{10}} \right)^{-1/3}. \quad (4.36)$$

On the other hand, if we take  $\sigma = 5/2$  and  $\rho = 8$  we obtain two solutions both lying inside the Kähler cone:

$$\tau = 3(5 + \sqrt{10}), \quad t = \frac{1}{60}(65 + 17\sqrt{10}),$$

$$z = \left( \frac{2}{9(3627 + 1121\sqrt{10})} \right)^{1/3},$$

and 
$$\tau = 3(5 - \sqrt{10}), \quad t = \frac{1}{60}(65 - 17\sqrt{10}),$$

$$z = \left( \frac{2}{9(3627 - 1121\sqrt{10})} \right)^{1/3}. \quad (4.37)$$

One distinguished feature is the existence of two distinct solutions for a given value of  $\sigma$  and  $\rho$  in the range  $2 < \sigma \leq 3$  and  $\rho > \rho_+$ . It is rather interesting to find multiple solutions preserving supersymmetry for the same set of charges in our model. Such examples were constructed first in the case of five dimensional supergravity theories arising from the compactification of M-theory on two parameter Calabi-Yau manifolds. It was later realized that the multiple solutions lie in different disconnected branches of the moduli space. While the examples studied in [14] admitted multiple non-BPS attractors, the BPS solutions for a given set of charges were all unique. Though multiple non-BPS attractors are found to occur in many supergravity theories, the existence of multiple BPS attractors seems quite exceptional.

## V. NON-BPS BLACK HOLES

We will now turn our attention to non-BPS black holes in the three parameter Calabi-Yau models. Thus, we need to analyze the equation of motion

$$8ZX_K + C_{KLM}(C^{IL}C^{JM} - C^{IJ}t^Lt^M)X_I X_J = 0, \quad (5.1)$$

with  $X_I \neq 0$ . We need to keep in mind that  $X_I$ 's satisfy the constraint (2.13),  $t^I X_I = 0$ . Setting  $X_I = \hat{X} \tilde{X}_I$  in (2.14), we obtain

$$\hat{X} = -\frac{8ZC^{IJ}\tilde{X}_I\tilde{X}_J}{C_{KLM}C^{KP}C^{LQ}C^{MN}\tilde{X}_P\tilde{X}_Q\tilde{X}_N}. \quad (5.2)$$

Using the above in the definition of  $X_I$  from (2.11), we find

$$q_I = Z \left( C_{IJ}t^J - \frac{8\tilde{X}_I C^{JK}\tilde{X}_J\tilde{X}_K}{C_{KLM}C^{KP}C^{LQ}C^{MN}\tilde{X}_P\tilde{X}_Q\tilde{X}_N} \right). \quad (5.3)$$

In terms of the charge ratios  $\rho = q_1/q_3$  and  $\sigma = q_2/q_3$  the above equation can be rewritten as

$$\rho = \frac{C_{1J}t^J C_{KLM}C^{KP}C^{LQ}C^{MN}\tilde{X}_P\tilde{X}_Q\tilde{X}_N - 8\tilde{X}_1 C^{JK}\tilde{X}_J\tilde{X}_K}{C_{3J}t^J C_{KLM}C^{KP}C^{LQ}C^{MN}\tilde{X}_P\tilde{X}_Q\tilde{X}_N - 8\tilde{X}_3 C^{JK}\tilde{X}_J\tilde{X}_K}, \quad (5.4)$$



$$\sigma = \frac{C_{2J} t^J C_{KLM} C^{KP} C^{LQ} C^{MN} \tilde{X}_P \tilde{X}_Q \tilde{X}_N - 8 \tilde{X}_2 C^{JK} \tilde{X}_J \tilde{X}_K}{C_{3J} t^J C_{KLM} C^{KP} C^{LQ} C^{MN} \tilde{X}_P \tilde{X}_Q \tilde{X}_N - 8 \tilde{X}_3 C^{JK} \tilde{X}_J \tilde{X}_K}. \quad (5.5)$$

With  $\tilde{X}_I$  being algebraic functions of  $t^I$  the right-hand sides of the above equations are only functions of the moduli. A consistent solution to the above conditions leads a non-BPS black hole. To find whether the resulting configuration is stable, we need to consider the recombination factor [10]. The recombination factor  $R$  is defined as the ratio of the black hole mass to the mass of the  $M2$ -brane wrapping the minimum piece-wise calibrated curve in the same homology class as the nonholomorphic curve corresponding to the black hole:

$$R = \frac{M_C}{M_{C^U}}, \quad (5.6)$$

where  $M_C$  is the mass of the  $M2$  brane wrapping the nonholomorphic curve  $C$  and  $M_{C^U}$  is the mass of the  $M2$  brane wrapping the minimum volume piece-wise calibrated curve  $C^U$  in the homology class  $[C]$ . The mass of the non-BPS black hole is given by  $M_C = \sqrt{V_{\text{cr}}}$ , the square root of the black hole potential at the critical point. On the other hand, if  $C = \sum \alpha_I C^I$ , then  $M_{C^U} = \sum |\alpha_I| t^I$ . Thus,

$$R = \frac{\sqrt{V_{\text{cr}}}}{\sum |\alpha_I| t^I}. \quad (5.7)$$

If this quantity is greater than one, the black hole becomes unstable and decays into the constituent BPS/non-BPS pairs. Whereas, for  $R < 1$  recombination of the brane/antibrane pairs takes place and the non-BPS black hole becomes stable [10].

Let us now focus on the constraint (2.13). In the case of two parameter Calabi-Yau models [14] it took the form  $\tilde{X}_1 x + \tilde{X}_2 y = 0$ . Thus, for the two parameter case it was possible to obtain the expressions for  $X_I$  uniquely upon solving this constraint. However, this is not the case for models with  $h_{1,1} > 2$ . In the present case the constraint takes the form  $\tilde{X}_1 x + \tilde{X}_2 y + \tilde{X}_3 z = 0$ . In terms of the rescaled coordinates we have  $\tilde{X}_1 \tau + \tilde{X}_2 t + \tilde{X}_3 = 0$ , and hence we can at most express  $\tilde{X}_3$  in terms of  $t^I$  and  $\tilde{X}_1, \tilde{X}_2$ . Thus, to obtain these quantities we need to solve the full equations of motion. In the following we will consider examples of three parameter models where we will explicitly solve the equations of motion to obtain the non-BPS attractors.

### A. Examples

We will now consider non-BPS attractors for the both the examples considered in the previous section. Let us first consider the first example, say the model 1. We need the explicit expression for the black hole effective potential to obtain the non-BPS solutions. Substituting the intersection numbers for the model 1 in (3.8) we find

$$V = \frac{3}{4y(y+z)(x+2y-2z)} (v_{11} q_1^2 + v_{22} q_2^2 + v_{33} q_3^2 + 2v_{12} q_1 q_2 + 2v_{23} q_2 q_3 + 2v_{31} q_3 q_1), \quad (5.8)$$

where the functions  $v_{ij}$  are defined as follows

$$\begin{aligned} v_{11} &= 2x^3 y(y+z) + x^2(4y^3 - 4yz^2 + 1) + 8x(y-z) + 16(3y^2 + z^2), \\ v_{22} &= y^2(2xy(y+z) + 4y^3 - 4yz^2 + 1), \\ v_{33} &= 2y^2(xz^2 + 2) + y(2xz^3 - 4z^4 + 4z) + 4y^3 z^2 + z^2, \\ v_{12} &= y(2x^2 y(y+z) + x(4y^3 - 4yz^2 - 1) - 8y), \\ v_{23} &= y(2xy^2 z + y(2xz^2 - 4z^3 - 2) + 4y^3 z - z), \\ v_{31} &= 2y^2(x^2 z + 6) + 2yz(x^2 z - 2xz^2 + 4) + 4xy^3 z + z(4z - x). \end{aligned} \quad (5.9)$$

The constraint on the volume (2.2) for the Calabi-Yau manifold  $\mathcal{M}$  becomes

$$2xy^2 + 2xyz + 4y^3 - 4yz^2 = 1. \quad (5.10)$$

In order to obtain the critical points, we need to extremize the black hole effective potential (5.8) using the method of Lagrange multiplier to incorporate the constraint (5.10) on the scalar fields. Upon eliminating the Lagrange multiplier we obtain two independent equations which after some simplifications take the form

$$\begin{aligned}
& q_1^2 f_{11} + q_2^2 f_{22} + 2q_3^2 y(y+z)(2y+z) + f_{12} q_1 q_2 + f_{23} q_2 q_3 + f_{31} q_3 q_1 = 0, \\
& (q_1(2x^2 y(y+z) + x(4y^3 - 4yz^2 + 1) + 8y) + q_2 y(2xy(y+z) + 4y^3 - 4yz^2 - 1) \\
& + q_3(2xy^2 z + 2y(xz^2 - 2z^3 + 1) + 4y^3 z + z))(q_1(x-4z) - q_3(y+z)) = 0.
\end{aligned} \tag{5.11}$$

The functions  $f_{ij}$  are defined as

$$\begin{aligned}
f_{11} &= 2x^3 y(2y^2 + 3yz + z^2) + x^2(20y^4 + 16y^3 z - 12y^2 z^2 + y(2 - 8z^3) + z) \\
&+ 2x(12y^5 - 16y^3 z^2 + 5y^2 + 4yz(z^3 - 1) - 3z^2) - 8(3y^3 + 9y^2 z + yz^2 - z^3), \\
f_{22} &= y^2(y+z)(2xy(y+z) + 4y^3 - 4yz^2 + 1), \\
f_{12} &= y(2x^2 y^2(y+z) + xy(16y^3 + 12y^2 z - 8yz^2 - 4z^3 - 1) + 2(12y^5 - 16y^3 z^2 + 5y^2 + 4yz(z^3 + 2) + z^2)), \\
f_{23} &= y(y+z)(2xy^2 z + 2xyz^2 + 4y^3 z - 4y(z^3 + 1) - z), \\
f_{31} &= 4y^3(x^2 z + 4xz^2 - 8z^3 - 6) - 2y^2 z(-3x^2 z + 6xz^2 + 19) + 2yz(x^2 z^2 - 4xz^3 - x + 4z^4 - 4z) \\
&+ 20xy^4 z + z^2(2z - x) + 24y^5 z.
\end{aligned} \tag{5.12}$$

We can rewrite these equations in terms of the inhomogeneous coordinates and the charge ratios and eliminate  $z$  using the constraint (5.10). The equations motion simplify remarkably to have the form

$$\begin{aligned}
& (\rho\tau + 4\rho t + t + 1)(\rho(\tau - 4) - t - 1) = 0, \\
& t^3 g_1 + t^2(g_2 - 8t\rho^2) + t(4\rho^2 + 4\rho + 1) - 2t\rho^2(\tau - 2) - \rho^2(\tau - 2)^2 = 0,
\end{aligned} \tag{5.13}$$

where  $g_1$  and  $g_2$  are functions of the charge ratios  $\rho$  and  $\sigma$  with the expression

$$g_1 = 12\rho^2 + \rho(12 - 8\sigma) + \sigma^2 - 2\sigma + 2, \quad g_2 = 36\rho^2 - 8\rho(\sigma - 2) + \sigma^2 - 2\sigma + 3. \tag{5.14}$$

It is indeed possible to solve these equations exactly to obtain the inhomogeneous coordinates in terms of the charge ratios. They admit four independent solutions. They are given as

$$\tau = -\frac{8\rho^2 + 8\rho - \sigma + 1}{\rho(2\rho - \sigma)}, \quad t = \frac{2\rho + 1}{2\rho - \sigma}, \tag{5.15}$$

$$\tau = \frac{8\rho^2 + \sigma - 1}{\rho(6\rho - \sigma + 2)}, \quad t = -\frac{2\rho + 1}{6\rho - \sigma + 2}, \tag{5.16}$$

$$\tau = \frac{8\rho^2 - 4\rho\sigma + 4\rho - \sigma + 1}{2\rho^2 - \rho\sigma}, \quad t = \frac{2\rho + 1}{2\rho - \sigma}, \tag{5.17}$$

$$\tau = \frac{24\rho^2 - 4\rho(\sigma - 3) - \sigma + 1}{\rho(6\rho - \sigma + 2)}, \quad t = -\frac{2\rho + 1}{6\rho - \sigma + 2}. \tag{5.18}$$

The last of these solutions corresponds to BPS black holes. They have been analyzed in detail in Sec. IV. On the other hand, the first three solutions do not satisfy the BPS equations. They corresponds to non-BPS attractors.

We need to make sure that the non-BPS solutions lie within the Kähler cone. From the expression of the Kähler cone matrix we observe that the values of  $t$  and  $\tau - 2$  must be positive. Let us analyze this condition for the first solution given in (5.15). We find

$$\frac{2\rho + 1}{2\rho - \sigma} > 0 \quad \text{and} \quad \frac{(2\rho + 1)(6\rho - \sigma + 1)}{\rho(2\rho - \sigma)} < 0. \tag{5.19}$$

Further, we consider the combination  $(t + 1)(\tau + 2t - 2)$  which is positive inside the Kähler cone. For (5.15), this implies  $\rho(2\rho + 1) < 0$ . Thus, the value of  $\rho$  must lie in the range  $-1/2 < \rho < 0$ . Since  $2\rho + 1$  is positive, the first inequality

in (5.19) implies  $2\rho - \sigma > 0$  and hence  $\sigma < 2\rho$ . The second inequality in (5.19) now implies  $\sigma < 6\rho + 1$ . Thus, the solution (5.15) remains inside the Kähler cone provided  $-1/2 < \rho < 0$  and  $\sigma < \min\{2\rho, 6\rho + 1\}$ .

We will now focus on the Kähler cone condition for the solution (5.16). A similar analysis tells that once again the values of  $\rho$  lies in the range  $-1/2 < \rho < 0$ . Requiring  $t > 0$  for a given  $\rho$  in this range now gives the bound  $\sigma > 6\rho + 2$ . Requiring  $\tau - 2 > 0$  gives  $\sigma > 2\rho + 1$ . Thus, the solution (5.16) lies inside the Kähler cone provided  $-1/2 < \rho < 0$  and  $\sigma > \max\{2\rho + 1, 6\rho + 2\}$ . Finally, let us consider the

solution (5.17). In this case  $\rho$  takes values in the range  $\rho > 0$  or  $\rho < -1/2$ . For  $\rho > 0$  we must have  $\sigma < 2\rho$  and for  $\rho < -1/2$  the value of  $\sigma$  lies in the range  $\sigma > 2\rho + 1$ . For these values of  $\rho$  and  $\sigma$  the solution (5.17) remain inside the Kähler cone. Further, these bounds ensure that all the four branches of solutions as given in (5.15)–(5.18) are mutually exclusive from each other. Thus, in this model both the BPS as well as non-BPS attractors are unique.

Let us now turn our attention to the second model consider in Sec. IV. The black hole effective potential (3.8) for this model takes the form

$$V = \frac{3q_1}{2x}(q_1x^3 + 2x^2(q_2y + q_3z) - q_2) + \frac{1}{8x^2(x-9z)}(q_2^2V_3 + q_2q_3V_2 + q_3^2V_1). \quad (5.20)$$

where, for easy reading we have introduced the functions

$$\begin{aligned} V_1 &= 4x(3xz^2 - 27z^3 + 1), \\ V_2 &= 4x(6x^2yz - 54xyz^2 - x + 3z), \\ V_3 &= 12x^3y^2 - x^2(108y^2z - 19) + 3x(2y - 55z) - 18z(3y + z). \end{aligned} \quad (5.21)$$

The constraint on the volume (2.2) becomes

$$2x^3 + x^2(2y + z) - 3xz^2 + 9z^3 = 1. \quad (5.22)$$

The equations of motion is obtained upon extremizing the potential (5.20) subject to the constraint (5.22). We find

$$\begin{aligned} 24q_1^2x^5(x-9z)^2 - q_2f_3(x,y,z)(4x^2(q_1x + q_2y + q_3z) + q_2) + 4q_2q_3x^2f_1(x,y,z) \\ + 12q_1x^2(x-9z)^2(2q_2x^2y + q_2 + 2q_3x^2z) - q_2^2f_5(x,y,z) - 4q_3^2x^4 = 0, \end{aligned} \quad (5.23)$$

$$(q_2f_1(x,y,z) - 2q_3x^2)(2x^2(2q_1x(x-9z)^2 + q_3f_2(x,y,z)) + q_2f_4(x,y,z)) = 0. \quad (5.24)$$

In the above the functions  $f_1, \dots, f_5$  are defined as follows

$$\begin{aligned} f_1(x,y,z) &= x^2 - 6xz + 27z^2, \\ f_2(x,y,z) &= 2x^2z - 36xz^2 + 162z^3 + 3, \\ f_3(x,y,z) &= 3(x-9z)^2(6x^2 + 2x(2y+z) - 3z^2), \\ f_4(x,y,z) &= 4x^4y - 72x^3yz + x^2(324yz^2 - 1) - 18xz + 81z^2, \\ f_5(x,y,z) &= x(19x^3 + 6x^2(2y - 55z) - 27xz(8y - 53z) + 324z^2(3y + z)). \end{aligned} \quad (5.25)$$

We express these equations in terms of the rescaled variables  $\tau = x/z, t = y/z$  and eliminate  $z$  using (5.22) to obtain

$$\begin{aligned} 4\tau^4(2\tau^3 + (2t+1)\tau^2 - 3\tau + 9) - 12\rho(\tau-9)^2\tau^2(2\tau^2(1+\rho\tau) - \sigma(4\tau^3 + \tau^2 - 9)) \\ - 4\sigma\tau^2(2\tau^5 + (2t-29)\tau^4 + (363-24t)\tau^3 + 9(30t-143)\tau^2 - 27(36t+29)\tau + 972) \\ + \sigma^2(74\tau^7 + (96t^2 - 3408t + 4785)\tau^5 - 9(192t^2 - 1588t - 777)\tau^4 + 54(144t^2 + 148t - 271)\tau^3 \\ - (1259 - 194t)\tau^6 - 81(174t - 263)\tau^2 + 2187(8t+5)\tau - 6561) = 0, \end{aligned} \quad (5.26)$$

and

$$(2\tau^2 - \sigma(\tau^2 - 6\tau + 27))(2\tau^2(6\tau^3 + (6t + 5)\tau^2 - 45\tau + 189) + 4\rho(\tau - 9)^2\tau^3 - \sigma(2\tau^5 - (2t - 37)\tau^4 + 3(36t - 49)\tau^3 - 18(27t + 7)\tau^2 + 405\tau - 729)) = 0. \quad (5.27)$$

Even though these equations look complicated, it is indeed to solve the inverse problem exactly to express the charge ratios in terms of the inhomogeneous coordinates  $(\tau, t)$ . We find three independent solutions:

$$\rho = \frac{6\tau^2 + (4t + 2)\tau - 3}{\tau^2 - 6\tau + 27}, \quad \sigma = \frac{2\tau^2}{\tau^2 - 6\tau + 27}, \quad (5.28)$$

$$\rho = -\frac{2\tau^3 + 2(2t + 1)\tau^2 - 9\tau + 36}{\tau(\tau^2 - 6\tau + 27)}, \quad \sigma = \frac{2\tau^2}{\tau^2 - 6\tau + 27} \quad (5.29)$$

and

$$\rho = -\frac{328\tau^5 + 36(6t^2 + 4t - 63)\tau^3 + (548t + 310)\tau^4 + (9981 - 1134t)\tau^2 + 81(84t + 23)\tau + 729}{92\tau^5 + 3(30t - 763)\tau^4 - 81(28t - 121)\tau^3 + 162(63t + 19)\tau^2 - 3645\tau + 6561}$$

$$\sigma = -\frac{2\tau^2(52\tau^3 + 27(2t + 3)\tau^2 - 567\tau + 1701)}{92\tau^5 + 3(30t - 763)\tau^4 - 81(28t - 121)\tau^3 + 162(63t + 19)\tau^2 - 3645\tau + 6561} \quad (5.30)$$

The first solution (5.28) corresponds to BPS black holes which has been considered in Sec. IV. On the other hand solutions obtained in (5.29) and (5.30) give rise to non-BPS black holes. We will now analyze them in detail. Consider first (5.29). We can solve them to obtain analytic expressions for the inhomogeneous coordinates  $(\tau, t)$ . Denoting

$$\tau_{\pm} = \frac{3(\sigma \pm \sqrt{2\sigma(3 - \sigma)})}{(\sigma - 2)},$$

$$t_{\pm} = \frac{1}{36(\sigma - 2)^3\sigma} (12(405\rho - 11)\sigma^2 - 8(2187\rho + 31)\sigma - 59\sigma^4 + 222\sigma^3 + 192 \mp \sqrt{2\sigma(3 - \sigma)}(972\rho\sigma + 5832\rho + 55\sigma^3 - 222\sigma^2 + 228\sigma - 8)), \quad (5.31)$$

there are two independent solutions  $(\tau_+, t_+)$  and  $(\tau_-, t_-)$ . The expression for  $\tau$  in these solutions remain the same as that of BPS black holes as given in (4.27). Thus, from the discussion followed by (4.33) we understand that requiring  $\tau_-$  to lie inside the Kähler cone for the solution  $(\tau_-, t_-)$  gives rise to the constraint  $1 < \sigma \leq 3$  for the possible values of  $\sigma$ . Further, introducing  $\rho_{\pm}$  as

$$\rho_{\pm} = \frac{1}{26244\sigma} (\sigma(185\sigma^2 - 948\sigma - 396) \pm 2\sqrt{2\sigma(3 - \sigma)}(167\sigma^2 + 18\sigma + 72)),$$

we find that the value  $t_-$  in the solution  $(\tau_-, t_-)$  remains positive if  $\rho < \rho_-$ . At  $\sigma = 3$ ,  $\rho_-$  takes its maximum possible value  $\rho_-^m = -175/2916$ . Thus, the non-BPS configurations  $(\tau_-, t_-)$  exist for  $1 < \sigma \leq 3$  and  $\rho < -175/2916$ . Let us now focus on the solution described by  $(\tau_+, t_+)$ . In this case, for  $2 < \sigma \leq 3$  the value of  $\tau_+$  remains greater than 3. Requiring  $t_+ > 0$  in this solution, we find that  $\rho$  must satisfy the upper bound  $\rho < \rho_+$ . From the expression for  $\rho_+$  we find that  $\rho_+ \leq 0$  throughout with the equality holding at

$\sigma = 2$ . Thus, this branch exists when  $2 < \sigma \leq 3$  and  $\rho < 0$ . Further, we notice that  $\rho_- \leq \rho_+$  in the range  $2 < \sigma \leq 3$ . Thus, for  $2 < \sigma \leq 3$  and  $\rho_- < \rho < \rho_+$  only  $(\tau_+, t_+)$  lies within the Kähler cone whereas, for  $\rho < \rho_-$  both the solutions survive.

Before we turn our attention to (5.30), we would like to compare the BPS and non-BPS solutions we have obtained so far. Though both the set of solutions exist only when  $1 < \sigma \leq 3$ , the range of  $\rho$  is entirely different. While, for the BPS solutions the minimum possible value of  $\rho$  is  $19/6$ , for the non-BPS solutions  $\rho$  must take negative values. Thus the BPS solutions obtained from (5.28) and non-BPS solutions derived from (5.29) do not coexist simultaneously.

We will now consider (5.30). This involves coupled equations of degree five in  $(\tau, t)$  and hence it is not possible to obtain an exact analytical expression for these variables in terms of  $(\rho, \sigma)$ . Nevertheless, it is possible to obtain the range of charge ratios which admit attractor solutions lying inside the Kähler cone. First thing to notice is that there exist curves of singularities in the moduli space which do not correspond to any possible extremal black hole

configuration for finite values of black hole charges. These curves are obtained by setting the denominators in the expressions for  $\rho$  and  $\sigma$  in (5.30) to zero. We find

$$92\tau^5 + 3(30t - 763)\tau^4 - 81(28t - 121)\tau^3 + 162(63t + 19)\tau^2 - 3645\tau + 6561 = 0. \quad (5.32)$$

This equation can be rewritten as

$$t = -\frac{92\tau^5 - 2289\tau^4 + 9801\tau^3 + 3078\tau^2 - 3645\tau + 6561}{18\tau^2(5\tau^2 - 126\tau + 567)}. \quad (5.33)$$

The above expression has two poles as well as two zeros. Denote the poles as  $\tau_{p1}, \tau_{p2}$  and the zeros as  $\tau_{z1}, \tau_{z2}$ . The values of  $\tau_{p1}$  and  $\tau_{p2}$  are

$$\tau_{p1} = \frac{9}{5}(7 - \sqrt{14}) \simeq 5.865, \quad \tau_{p2} = \frac{9}{5}(7 + \sqrt{14}) \simeq 19.335,$$

and the zeros  $\tau_{z1}, \tau_{z2}$  are approximately  $\tau_{z1} \simeq 5.859, \tau_{z2} \simeq 19.266$ . The value of  $t$  as given in (5.33) remains positive in the intervals  $(\tau_{z1}, \tau_{p1})$  and  $(\tau_{z2}, \tau_{p2})$ . Thus, there are two curves of singularities. They form a pair of almost straight lines which start respectively from  $\tau_{z1}$  and  $\tau_{z2}$  at  $t = 0$  and asymptote to  $\tau = \tau_{p1}$  and  $\tau = \tau_{p2}$  lines as  $z \rightarrow \infty$ . Any point inside the Kähler cone which does not lie on either of these two curves correspond to an extremal non-BPS black hole configuration for some suitably chosen charges.

The singularity curves naturally divide the moduli space into three regions. We denote the region bounded by the singularity curve asymptote to the line  $\tau = \tau_{p1}$  and the  $\tau = 3$  boundary of the Kähler cone as region 1, the region bounded by the curve asymptote to the line  $\tau = \tau_{p2}$  and the boundary  $\tau = \infty$  as region 2 and the region bounded by the two curves of singularities as region 3. If we treat  $\sigma$  and  $\rho$  as functions of  $(t, \tau)$ , then they do not possess any extremum in regions 1 and 2. In region 1,  $\sigma$  takes a maximum value  $-79/257$  at the boundary point  $t = 0, \tau = 3$ . As we move away from this point,  $\sigma$  becomes more and more negative and  $\sigma \rightarrow -\infty$  as we approach the singularity curve. In region 2,  $\sigma$  attains a maximum value of  $-26/23$  in the limit  $\tau \rightarrow \infty$ . It takes a smaller value for any point interior to this region and as we approach the singularity curve,  $\sigma \rightarrow -\infty$ . In region 3,  $\sigma \rightarrow \infty$  as we approach either of the singularity curves from an interior point of this region. However, it remains positive throughout inside the region 3 and hence form a valley shaped surface. To find the minimum value of  $\sigma$  in this region we set both the partial derivatives  $\frac{\partial \sigma}{\partial t}$  and  $\frac{\partial \sigma}{\partial \tau}$  to zero to obtain:

$$(\tau - 9)^5 = 0$$

and

$$\begin{aligned} &(\tau - 9)(729(28t^2 + 36t + 143)\tau^4 + 8(6t + 2635)\tau^6 \\ &+ 144(276t + 17)\tau^5 - 1458(30t + 217)\tau^3 \\ &+ 6561(4t + 13)\tau^2 - 275562\tau + 413343) = 0. \end{aligned}$$

Thus  $\sigma$  has a line of minima given by  $\tau = 9$ , with the minimum value  $\sigma_m = 3$ .

We now focus on the range of values for  $\rho$  that admits attractor solutions. In region 1 as well as region 2 it does not admit an extremum. At the boundary point  $t = 0, \tau = 3$  of region 1 it takes the maximum value  $\rho = -575/514$ . As we move away from this point, it becomes more negative and diverges as we approach the singularity curve. Similarly, in region 2, it has a maximum value  $\rho = -82/23$  in the limit  $\tau \rightarrow \infty$ . It becomes more negative at finite  $\tau$  and as we approach the singularity curve,  $\rho$  diverges. In the interior of region 3,  $\rho$  takes positive values and  $\rho \rightarrow \infty$  as we approach the singularity curves from any point in the interior. To find the minimum value of  $\rho$  in this region, we set  $\frac{\partial \rho}{\partial t}$  and  $\frac{\partial \rho}{\partial \tau}$  to zero. A numerical computation indicates that these equations do not admit any solution in the interior of region 3. For any fixed  $t$  it admits a minimum for some  $\tau$ . The value of this minimum decreases with  $t$ . Thus, the functional form of  $\rho$  defines a valley which slopes downward toward smaller values of  $t$ . To find the smallest allowed value of  $\rho$ , we set  $t = 0$  in it and extremize. We find

$$\begin{aligned} &(1640\tau^4 + 1240\tau^3 - 6804\tau^2 + 19962\tau + 1863) \\ &\times (92\tau^5 - 2289\tau^4 + 9801\tau^3 + 3078\tau^2 - 3645\tau + 6561) \\ &- (460\tau^4 - 9156\tau^3 + 29403\tau^2 + 6156\tau - 3645)(328\tau^5 \\ &+ 310\tau^4 - 2268\tau^3 + 9981\tau^2 + 1863\tau + 729) = 0. \quad (5.34) \end{aligned}$$

This admits a unique solution  $\tau_m$  in region 3. Numerically we find  $\tau_m \simeq 9.03$ . The value of  $\rho$  corresponding to this point is  $\rho_m \simeq 9.277$ .

From the above analysis we find that, for  $\sigma > 3$  and  $\rho > \rho_m$  we have multiple non-BPS solutions in region 3. If  $-26/23 < \sigma < -79/257$  and  $-82/23 < \rho < -575/514$  we have a unique non-BPS attractor in region 1 for a given set of charges. Finally, for  $\sigma < -26/23$  and  $\rho < -82/23$  we have two non-BPS attractors for a given set of charges one of which lies in region 1 and the other in region 2. No attractors exist for charges lying in the range  $-79/257 < \sigma < 3$  and  $-575/514 < \rho < \rho_m$ . Further, we note that since the above solutions exist only when  $\sigma > 3$  or  $\sigma < -79/257$ , whereas the solutions obtained from (5.28) and (5.29) exist only when  $1 < \sigma \leq 3$ , all the three set of solutions are mutually exclusive.

As an example, consider the values  $\sigma = 4, \rho = 16$ . It gives a pair of solutions for  $(\tau, t, z)$  with approximate values  $(7.101, 2.231, 10.225)$  and  $(12.281, 4.102, 17.682)$ ,

both lying in region 3. If we take  $\sigma = -2, \rho = -7$  we find one solution in region 1 with  $\tau \simeq 4.853$  and  $t \simeq 0.61$  and another in region 2 with  $\tau \simeq 55.008$  and  $t \simeq 10.363$ . In this case  $z$  takes the approximate values 6.506 and 73.587 respectively. On the other hand, for  $\sigma = -1, \rho = -7/2$  we find a unique solution in region 1 with  $\tau \simeq 4.298, t \simeq 0.383$  and  $z \simeq 5.724$ .

### B. Stability

Now we will analyze the stability of the non-BPS black holes obtained in the previous subsection. For this purpose we need to obtain the recombination factors of the respective black hole configurations. Let the non-BPS black hole results from wrapping a  $M2$  brane on a nonholomorphic curve  $C = \alpha_1 C^1 + \alpha_2 C^2 + \alpha_3 C^3$  of the Calabi-Yau manifold  $\mathcal{M}$ . The charges  $q_I$  of the black hole are given by

$$q_I = \int_C J_I = \alpha_1 C^1 \cdot J_I + \alpha_2 C^2 \cdot J_I + \alpha_3 C^3 \cdot J_I. \quad (5.35)$$

The intersection numbers  $C^I \cdot J_L$  can be obtained from the expression for the Kähler cone matrix (4.13) corresponding to the THCY manifold  $\mathcal{M}$ . We find

$$q_1 = \alpha_1 - 2\alpha_3, \quad q_2 = \alpha_2, \quad q_3 = \alpha_3. \quad (5.36)$$

From the above we find the coefficients  $\alpha_I$  in terms of the black hole charges  $q_I$  as  $\alpha_1 = q_1 + 2q_3 = (2\rho + 1)q_3, \alpha_2 = q_2 = \sigma q_3$  and  $\alpha_3 = q_3$ . Thus the recombination factor (5.7) corresponding to the non-BPS black holes in model 1 have the expression

$$R = \frac{\sqrt{V_{\text{cr}}}}{z|q_3|(|(2\rho + 1)|\tau + |\sigma|t + 1)}. \quad (5.37)$$

Here  $V_{\text{cr}}$  is the value of the effective black hole potential at the critical point. Substituting the expression for the effective black hole potential (5.8), using the volume constraint (5.10) and simplifying, we find

$$R = \frac{\sqrt{3(\rho^2(\tau^2 - 4\tau + 8) + 4\rho + t^2(24\rho^2 + \rho(12 - 8\sigma) + \sigma^2 - 2\sigma + 2) + t(4\rho^2\tau + 8\rho + 2) + 1)}}{(|(2\rho + 1)|\tau + |\sigma|t + 1)} \quad (5.38)$$

We need to substitute the solutions in the three branches of non-BPS black holes to obtain the corresponding recombination factors in each of the cases. Consider the solution (5.15) first. Recall that, the allowed values of  $\rho$  and  $\sigma$  for this solution are negative, whereas  $2\rho + 1 > 0$ . Keeping this in mind and substituting (5.15) in (5.38) we find the recombination factor to have the form

$$R = -\frac{3\rho(2\rho + 1)(4\rho - \sigma + 1)}{16\rho^3 + 2\rho^2(\sigma + 11) + 10\rho - \sigma + 1}. \quad (5.39)$$

The black hole becomes unstable when  $R > 1$ . This happens for

$$\sigma > \frac{40\rho^3 + 40\rho^2 + 13\rho + 1}{4\rho^2 + 3\rho + 1}. \quad (5.40)$$

However, recall that for the solution (5.15) to remain inside the Kähler cone we need to impose the bound  $\sigma < \min\{2\rho, 6\rho + 1\}$ . This may not be always compatible with (5.40). We find that (5.40) does not hold when  $\rho$  takes values in the range  $(\sqrt{17} - 9)/32 < \rho < 0$  or  $-1/2 < \rho < (\sqrt{17} - 9)/16$ . For these values of  $\rho$  the recombination factor  $R$  is always smaller than one and the corresponding black hole solutions are stable. For  $(\sqrt{17} - 9)/16 < \rho < (\sqrt{17} - 9)/32$  we can choose  $\sigma$  to satisfy (5.40). In that case the resulting non-BPS black holes become unstable. However, we can also choose  $\sigma$  not to satisfy this bound.

The non-BPS black holes for those values of  $\sigma$  remain stable against decay into constituent BPS/anti-BPS pairs.

Next consider the second branch of solutions given by (5.16). Here the charge ratios take values in the interval  $-1/2 < \rho < 0$  and  $\sigma > \max\{2\rho + 1, 6\rho + 2\}$ . Hence the values of  $\sigma$  and  $2\rho + 1$  always remain positive. Substituting (5.16) in (5.38) and simplifying we find

$$R = -\frac{3\rho(2\rho + 1)(4\rho - \sigma + 1)}{16\rho^3 - 2\rho^2(\sigma - 7) + \sigma - 1}. \quad (5.41)$$

In order to get  $R > 1$  the charge ratios need to satisfy the bound

$$\sigma > \frac{40\rho^3 + 32\rho^2 + 3\rho - 1}{8\rho^2 + 3\rho - 1}. \quad (5.42)$$

However, for  $-1/2 < \rho < 0$ , the right-hand side (rhs) of the above equation is always smaller than  $\max\{2\rho + 1, 6\rho + 2\}$ . Since the Kähler condition implies  $\sigma > \max\{2\rho + 1, 6\rho + 2\}$ , all such values of  $\sigma$  satisfy the bound (5.42). Thus, the recombination factor is always greater than one and hence the resulting non-BPS black holes in this branch are all unstable.

Finally, for the branch (5.17), the recombination factor takes the form

$$R = \left| \frac{3\rho(2\rho + 1)(4\rho - \sigma + 1)}{2\rho + 1|(8\rho^2 - 4\rho(\sigma - 1) - \sigma + 1) + \rho(2\rho|\sigma| + |\sigma| + 2\rho - \sigma)} \right|. \quad (5.43)$$

For this solution to be inside the Kähler cone we can have either  $\rho > 0, \sigma < 2\rho$  or  $\rho < -1/2, \sigma > 2\rho + 1$ . We will treat the stability conditions for  $\rho > 0, 0 < \sigma < 2\rho$  and  $\rho > 0, \sigma < 0$  separately. Consider first the case  $\rho > 0, 0 < \sigma < 2\rho$ . Analyzing the formula (5.43) we find that for  $\rho > (2 - \sqrt{2})^{1/3}(2^{1/3} + (2 + \sqrt{2})^{2/3})/4$  the value of the recombination factor always becomes greater than one irrespective of the value of  $\sigma$  and the black holes become unstable. However, for  $0 < \rho < (2 - \sqrt{2})^{1/3}(2^{1/3} + (2 + \sqrt{2})^{2/3})/4$  the black holes become unstable if  $\sigma > 1 - 8\rho^3/(3\rho + 1)$ , and stable if  $\sigma < \min\{2\rho, 1 - 8\rho^3/(3\rho + 1)\}$ . In the case  $\rho > 0, \sigma < 0$ , black holes become stable if  $\sigma < \min\{0, (1 + 3\rho - 8\rho^3)/(1 + 5\rho + 4\rho^2)\}$  and unstable otherwise. Similarly, for  $\rho < -1/2, \sigma > 0$  we find stable non-BPS black holes provided  $\sigma > \max\{0, (1 + 3\rho - 4\rho^2 - 8\rho^3)/(1 + 3\rho + 4\rho^2)\}$ . For  $\rho < -1/2, 2\rho + 1 < \sigma < 0$  there are no stable attractors if  $\rho < \rho_0$  where  $\rho_0 \simeq -0.776$  is a root of  $8\rho^3 + 4\rho^2 - 3\rho - 1 = 0$ . For  $\rho_0 < \rho < -1/2$  we have stable attractors if  $\sigma$  takes values in the interval  $\max\{2\rho + 1, -(8\rho^3 + 4\rho^2 - 3\rho - 1)/(\rho + 1)\}$ .

We will now analyze the stability of the non-BPS black holes in model 2. Let the corresponding  $M2$  brane wraps a

nonholomorphic curve  $C = \sum \alpha_I C^I$ . Using the expression for the Kähler cone matrix in (4.25), we find the charges  $q_I$  of the black hole to be

$$q_1 = \alpha_3, \quad q_2 = \alpha_1, \quad \text{and} \quad q_3 = \alpha_2 - 3\alpha_3. \quad (5.44)$$

Thus, the coefficients  $\alpha_I$  are given in terms of the charges  $q_I$  as  $\alpha_1 = q_2 = \sigma q_3, \alpha_2 = 3q_1 + q_3 = (3\rho + 1)q_3$  and  $\alpha_3 = q_1 = \rho q_3$ . The recombination factor (5.7) can be expressed as

$$R = \frac{\sqrt{V_{\text{cr}}}}{z|q_3|(|\sigma|\tau + |(3\rho + 1)|t + |\rho|)}. \quad (5.45)$$

Using the constraint (5.22) in (5.20), the recombination factor takes the form

$$R = \frac{1}{2\tau(|\sigma|\tau + |(3\rho + 1)|t + |\rho|)} \sqrt{\frac{\tilde{V}}{2(\tau - 9)}}, \quad (5.46)$$

where we have introduced

$$\begin{aligned} \tilde{V} = & \sigma^2(38\tau^5 - 311\tau^4 - 258\tau^3 + 24t^2(\tau - 9)\tau^2 + 648\tau^2 + 2t(25\tau^4 - 216\tau^3 - 54\tau^2 + 108\tau - 243) - 1431\tau - 162) \\ & + 4\tau^2(3\rho^2(\tau - 9)\tau^2 + 6\rho(\tau - 9)\tau + 2\tau^3 + (2t + 1)\tau^2 - 18) - 4\sigma\tau(3\rho(2\tau^4 - 17\tau^3 - 12\tau^2 + 36\tau - 81) \\ & + 2\tau^4 + (2t - 5)\tau^3 - 6(2t + 1)\tau^2 + 18(3t + 1)\tau - 27). \end{aligned} \quad (5.47)$$

The black hole becomes stable for  $R < 1$ . By directly substituting specific values of charges and the corresponding solutions  $t$  and  $\tau$  we find stable black holes for a wide range of charges. In the following we consider a class of configurations for stable as well as unstable black holes.

We choose a specific value of the charge ratio  $\sigma = 3/2$ . In this case, the equations of motion admit a unique solution given by  $(\tau_-, t_-)$  in (5.31). Substituting  $\sigma = 3/2$  in  $(\tau_-, t_-)$  we find the solution to have the simple form

$$\tau_- = 9(\sqrt{2} - 1) \quad \text{and} \quad t_- = \frac{1}{36} \left( 141 - 161\sqrt{2} \right) - 3(\sqrt{2} - 1)\rho. \quad (5.48)$$

For  $t_- > 0$  we need  $\rho$  to satisfy the bound  $\rho < -(181 + 20\sqrt{2})/108 \simeq -1.938$ . We substitute these values for  $\tau_-$  and  $t_-$  [and  $\sigma = 3/2$ ] in (5.46) to obtain the following simple expression for the recombination factor:

$$R = \frac{9(1 + \sqrt{2})\sqrt{11664(17 - 12\sqrt{2})\rho^2 + 216(1952\sqrt{2} - 2765)\rho - 317524\sqrt{2} + 449721}}{2(324(\sqrt{2} - 1)\rho^2 + (591\sqrt{2} - 567)\rho + 647\sqrt{2} - 627)}.$$

It can be easily verified that  $R < 1$  provided

$$\rho < -\frac{1}{216} \left( 367 + 8\sqrt{2} + \sqrt{5(28101 + 80\sqrt{2})} \right) \simeq -3.49. \quad (5.49)$$

Thus, for  $\sigma = 3/2$  we obtain non-BPS attractors as given by (5.48). The Kähler cone condition requires that  $\rho \lesssim -1.938$ . These non-BPS black holes remain unstable in the range  $-3.49 \lesssim \rho \lesssim -1.938$  and become stable when  $\rho \lesssim -3.49$ .

We will now take the value  $\sigma = 5/2$ . In this case there are two solutions  $(\tau_+, t_+)$  and  $(\tau_-, t_-)$  with

$$\tau_{\pm} = 3(5 \pm \sqrt{10}), \quad t_{\pm} = -\frac{1}{180} \left( 108(5 \pm \sqrt{10})\rho \pm 271\sqrt{10} + 1423 \right). \quad (5.50)$$

The solution  $(\tau_-, t_-)$  exists when  $\rho < -(4405 + 68\sqrt{10})/1620$  and the solution  $(\tau_+, t_+)$  exists when  $\rho < -(4405 - 68\sqrt{10})/1620$ . Thus, we have multiple solution for  $\rho < -(4405 + 68\sqrt{10})/1620$ . We can substitute these solutions in (5.46) to find the respective recombination factors

$$R_{\pm} = \frac{15\sqrt{5}\sqrt{6480(89 \pm 28\sqrt{10})\rho^2 - 216(13375 \pm 4208\sqrt{10})\rho \pm 1138324\sqrt{10} + 3618013}}{2(540(7 \pm 2\sqrt{10})\rho^2 + 3(3595 \pm 1026\sqrt{10})\rho \pm 5426\sqrt{10} + 19025)}$$

Introducing  $\rho_{s\pm}$  as

$$\rho_{s\pm} = -\frac{8695 \mp 8\sqrt{10} + \sqrt{87877865 \pm 72560\sqrt{10}}}{3240}$$

we find that  $R_{\pm} < 1$  provided  $\rho < \rho_{s\pm}$ . Hence, the solution  $(\tau_-, t_-)$  is unstable for  $\rho_{s-} < \rho < -(4405 + 68\sqrt{10})/1620$  and becomes stable for  $\rho < \rho_{s-}$  whereas the solution  $(\tau_+, t_+)$  is unstable for  $\rho_{s+} < \rho < -(4405 - 68\sqrt{10})/1620$  and becomes stable for  $\rho < \rho_{s+}$ . Since  $\rho_{s-} < \rho_{s+}$ , both the solutions in (5.50) become stable when  $\rho < \rho_{s-}$ .

We will now analyze the stability of solutions for (5.30). In this case it is not possible to obtain any analytical results. We can numerically solve the equations of motion for various choices of  $\rho$  and  $\sigma$  and obtain the recombination factor for each of the solutions. As we have noted previously, in this case there exist two singularity curves which divide the moduli space into three regions. We first consider  $\sigma > 3$  and  $\rho > \rho_m$  for which the solutions lie in region 3. We took the value  $\rho = 45$  and varied  $\sigma$  from 4 to 14. In each of these cases, there are two distinct solutions. Upon computing the recombination factor we observe that for a fixed  $\rho$  and for small values of  $\sigma$  the black holes

become stable. The recombination factor increases monotonically and the black holes become unstable for larger values of  $\sigma$ . We also observe that, for fixed values of  $(\rho, \sigma)$  with a smaller value  $\sigma$ , the recombination factors corresponding to the two distinct solutions almost coincide with each other. In the following, we plot the solutions for  $\tau$  and  $t$  in Fig. 1. We can clearly see two branches of solutions in both the cases. Since the recombination factors corresponding to the two branches of solutions are close to each other, we plot it for the lower branch of solutions. Further, we plot the difference of the two recombination factors separately (see Fig. 2).

We will now consider the solutions in regions 1 and 2. In this case, we have a unique non-BPS attractor in region 1 when  $\sigma$  and  $\rho$  lies in the range  $-26/23 < \sigma < -79/257$  and  $-82/23 < \rho < -575/514$  and multiple non-BPS attractors when  $\sigma < -26/23, \rho < -82/23$ . We will first focus on the unique solutions in region 1. We chose  $\sigma$  to be valued in the range  $-21/20 \leq \sigma \leq -11/20$  and  $\rho = -7/2$ . The resulting solution for  $\tau$  and  $t$  are plotted in Fig. 3. We notice that  $t$  monotonically increases with  $\sigma$ , while  $\tau$  decreases as we increase it. We have numerically computed the corresponding recombination factors (see Fig. 6). We find stable non-BPS black holes for smaller values of  $\sigma$ .

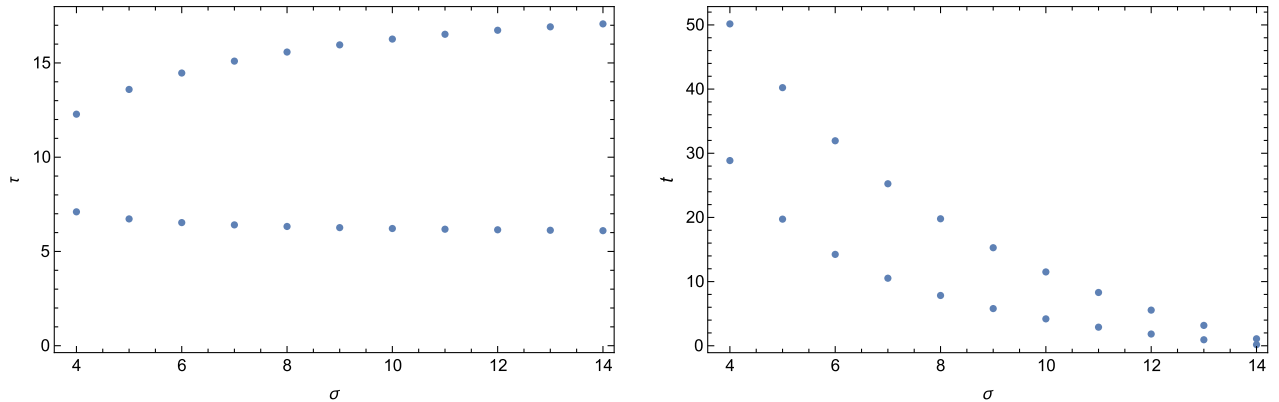


FIG. 1. Two branches of solutions for  $\tau$  and  $t$  with  $\rho = 45$  and  $4 \leq \sigma \leq 14$ .



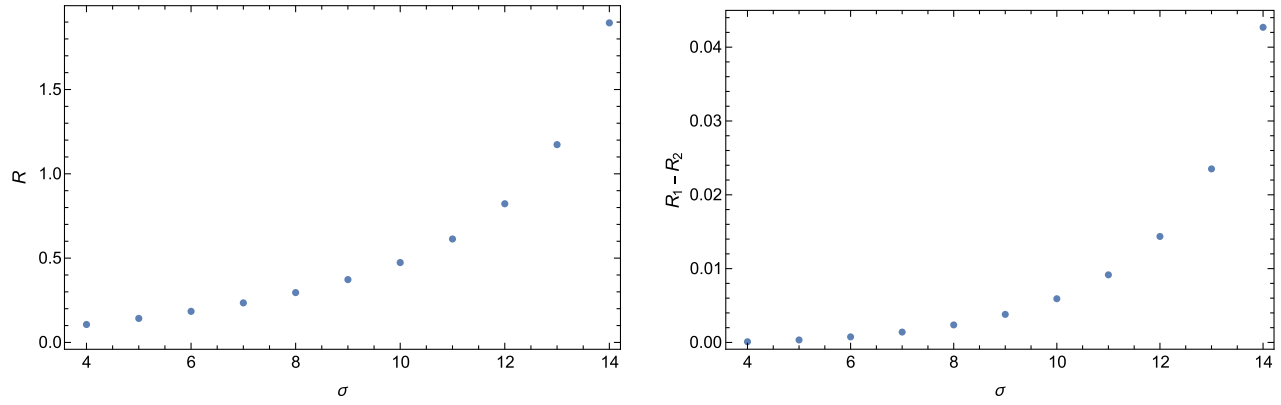


FIG. 2. Recombination factor for the lower branch of solutions and the difference of two recombination factors. The recombination factors take slightly higher values in the upper branch of solutions.

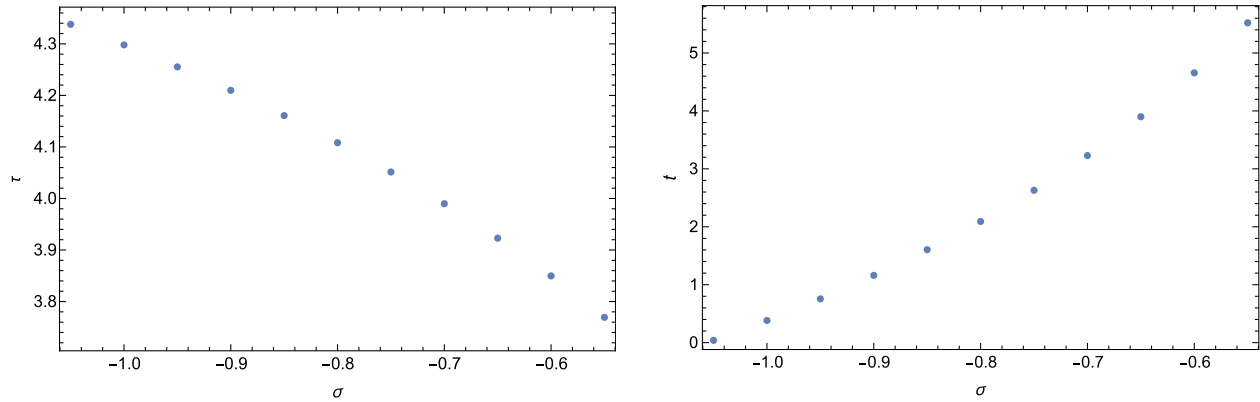


FIG. 3. Solutions for the inhomogeneous coordinates  $\tau$  and  $t$  in region 1 for  $\rho = -7/2$  and  $-21/20 \leq \sigma \leq -11/20$ .

Further, we choose the value  $\rho = -15$  for various  $\sigma$  in the range  $-23/5 \leq \sigma \leq -13/5$ . Multiple solutions occur for these values of the charge ratios. We find one solution in region 1 and the other in region 2. The solutions for  $(\tau, t)$  in region 1 are plotted in Fig. 4 and solutions for  $(\tau, t)$  in the region 2 are plotted in Fig. 5. The corresponding recombination factors are plotted in Fig. 6.

The lower curve in Fig. 6 corresponds to recombination factors in region 1 and upper curve in it corresponds to recombination factors in region 2. The black hole solutions with a larger value of  $\sigma$  remain stable. The value of  $R$  increases gradually as we decrease  $\sigma$  with a fixed value of  $\rho$  and the black holes become unstable after a critical value.

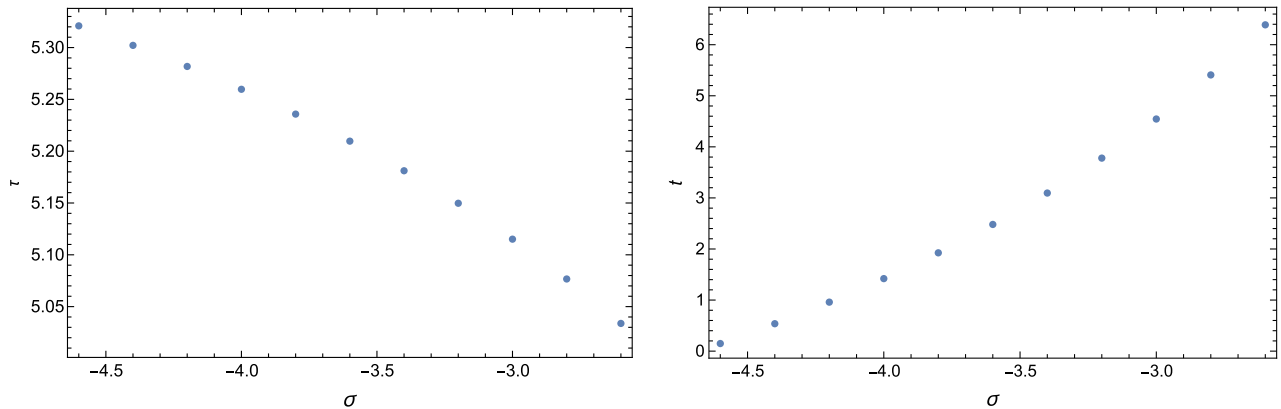
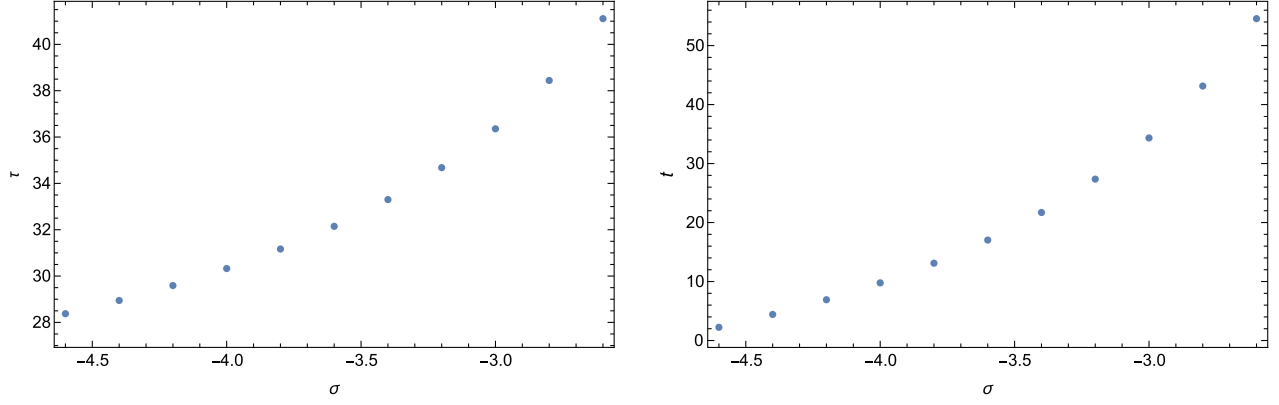
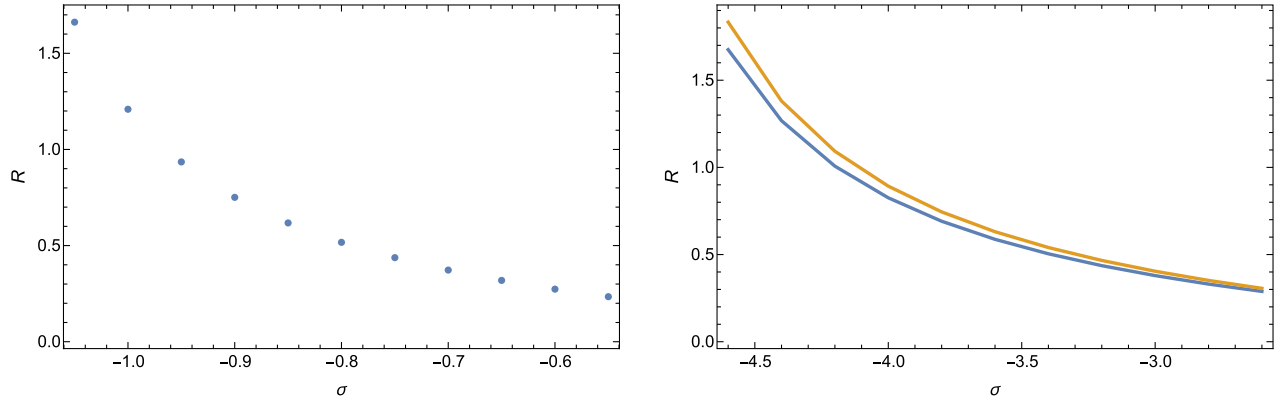


FIG. 4. Solutions for the inhomogeneous coordinates  $\tau$  and  $t$  in region 1 for  $\rho = -15$  and  $-23/5 \leq \sigma \leq -13/5$ .


 FIG. 5. Solutions for the inhomogeneous coordinates  $\tau$  and  $t$  in region 2 for  $\rho = -15$  and  $-23 \leq \sigma \leq -13/5$ .

 FIG. 6. Recombination factors for the above solutions. The figure in the left corresponds to recombination factors for solutions in region 1 with  $\rho = -7/2$  and  $-21/20 \leq \sigma \leq -11/20$ . The figure in right corresponds to recombination factors for the multiple solutions with  $\rho = -15$  and  $-23 \leq \sigma \leq -13/5$ .

## VI. NON-BPS BLACK STRINGS

We will now consider black strings in our supergravity theory. These are magnetically charged objects with charges  $p^I$ . They are obtained upon wrapping  $M5$  branes on a four cycle of the Calabi-Yau manifold. The central charge associated with the black string is given by

$$Z = C_{IJK} p^I t^J t^K. \quad (6.1)$$

The effective potential corresponding to the black string is

$$V = 3Z^2 - 2C_{IJ} p^I p^J. \quad (6.2)$$

To obtain the equation of motion, we need to extremize this effective black string potential. Note that the moduli  $t^I$  are constrained to satisfy (2.2). We can use the method of Lagrange multipliers to extremize the potential. The resulting equation of motion is given by

$$6Z(p^J - Zt^J) - C^{JK} C_{KLM} p^L p^M + C_{LM} p^L p^M t^J = 0. \quad (6.3)$$

Upon introducing  $X^I \equiv p^I - Zt^I$ , the above equation can be rewritten as [14]

$$4ZX^I + X^J X^K C_{JKL} (t^L t^I - C^{LI}) = 0. \quad (6.4)$$

Setting  $X^I = 0$  we obtain BPS solutions. Upon simplification, they take the form

$$t^I = \frac{p^I}{(C_{JKL} p^J p^K p^L)^{1/3}}. \quad (6.5)$$

Thus, for any five dimensional supergravity the resulting BPS black string solutions are unique. Solutions of the equation of motion (6.4) with  $X^I \neq 0$  correspond to non-BPS black strings.

For non-BPS black strings, using (2.2) we can show that  $X^I$  satisfies the constraint

$$C_{IJK} t^I t^J X^K = 0. \quad (6.6)$$

Multiplying  $X^I$  on (6.4) we can show that

$$4ZC_{IJ}X^IX^J - C_{IJK}X^IX^JX^K = 0. \quad (6.7) \quad \text{Similarly, using (3.2) we find}$$

Setting  $X^I = \check{X}\check{X}^I$  in the above we find

$$\check{X} = \frac{4ZC_{MN}\check{X}^M\check{X}^N}{C_{IJK}\check{X}^I\check{X}^J\check{X}^K}. \quad (6.8) \quad C_{IJ}p^I p^J = A_1(p^1)^2 + A_4(p^2)^2 + A_6(p^3)^2 + 2(A_2p^1 p^2 + A_3p^1 p^3 + A_5p^2 p^3). \quad (6.10)$$

and  $\check{X}^I$  satisfies the constraint  $C_{IJK}t^I t^J \check{X}^K = 0$

In the present work we will focus on three parameter models. Using the expression for  $C_{IJK}t^I t^J$  given in (3.5) we find the central charge (6.1) to have the form

$$Z = (A_1x + A_2y + A_3z)p^1 + (A_2x + A_4y + A_5z)p^2 + (A_3x + A_5y + A_6z)p^3. \quad (6.9)$$

Substituting these values in (6.2) we can obtain the expression for the black string effective potential. We will once again focus on the explicit examples we have considered in the previous sections to study BPS and non-BPS black holes. Let us consider the model 1 first. The effective black string potential for this model is given by

$$V = \frac{4}{3}(p^1y(y+z) + p^2x(2y+z) + 6p^2y^2 - 2p^2z^2 + p_3y(x-4z))^2 - \frac{4}{3}(p^1p^2(2y+z) + p^3y(p^1 - 2p^3) + (p^2)^2(x+6y) + p^2p^3(x-4z)) \quad (6.11)$$

Upon extremization with respect to the scalar fields  $x, y, z$  subject to the constraint (5.10) we find the equations of motion to be of the form

$$\begin{aligned} & (y+z)(p^2(p^1 - 4p^3) - 2(y(p^1 - 4p^3) + p^2(x-4z))(p^1y(y+z) + p^2x(2y+z) \\ & + 6p^2y^2 - 2p^2z^2 + p^3y(x-4z))) + (x-4z)(2(p^2(2y+z) + p^3y)(p^1y(y+z) \\ & + p^2x(2y+z) + 6p^2y^2 - 2p^2z^2 + p^3y(x-4z)) - p^2(p^2 + p^3)) = 0, \\ & y(x-4z)(2(p^1(2y+z) + 2p^2(x+6y) + p^3(x-4z))(p^1y(y+z) + p^2x(2y+z) \\ & + 6p^2y^2 - 2p^2z^2 + p^3y(x-4z)) - 2p^1p^2 - p^3(p^1 - 2p^3) - 6(p^2)^2) + (x(2y+z) \\ & + 6y^2 - 2z^2)(p^2(p^1 - 4p^3) - 2(y(p^1 - 4p^3) + p^2(x-4z))(p^1y(y+z) \\ & + p^2x(2y+z) + 6p^2y^2 - 2p^2z^2 + p^3y(x-4z))) = 0. \end{aligned} \quad (6.12)$$

As before we will introduce the inhomogeneous coordinates  $\tau = x/z, t = y/z$  and eliminate  $z$  using the constraint (5.10). In addition, we will rescale the magnetic charges  $p^I$  as  $p^1 = rp^3$  and  $p^2 = sp^3$ . The equations of motion (6.12) simplify a lot upon expressing in terms of the inhomogeneous coordinates  $\tau, t$  and charge ratios  $r, s$ . We find

$$\begin{aligned} & (rt + r - s\tau + 4s - 4t - \tau)(rt + r + 4st + s\tau + \tau - 4) = 0, \\ & t(\tau - 4)((2rt + r + 2s(6t + \tau) + \tau - 4)(t(rt + r + \tau - 4) + s(6t^2 + 2\tau t + \tau - 2)) \\ & - t(t+1)(2rs + r + 6s^2 - 2)(2t + \tau - 2)) + (6t^2 + 2\tau t + \tau - 2)((r-4)st(t+1) \\ & (2t + \tau - 2) - ((r-4)t + s(\tau - 4))(t(rt + r + \tau - 4) + s(6t^2 + 2\tau t + \tau - 2))) = 0. \end{aligned} \quad (6.13)$$

It is possible to solve the above equations exactly to find the attractor values of the moduli in terms of the magnetic charges. Apart from the BPS solution  $\tau = r, t = s$ , there are three additional solutions to the above equations. These solutions correspond to non-BPS black strings. They have the simple form

$$\tau = 4 - r - 4s, \quad t = s, \quad (6.14)$$

$$\tau = \frac{r+8s}{1+2s}, \quad t = -\frac{s}{1+2s}, \quad (6.15)$$

$$\tau = \frac{4-r+4s}{1+2s}, \quad t = -\frac{s}{1+2s}. \quad (6.16)$$

Requiring the solution to satisfy the Kähler cone condition  $\tau > 2$ ,  $t > 0$  we find the supersymmetric solutions for  $r > 2$ ,  $s > 0$ . For the first branch of non-BPS solutions (6.14), we have  $s > 0$ ,  $r < -2(2s-1)$ . For the second

branch (6.15) we have  $-1/2 < s < 0$  and  $r > 2(1-2s)$ . For the third branch  $-1/2 < s < 0$  and  $r < 2$ . All these branches of solutions are mutually exclusive from each other. Moreover, the resulting solution for a given set of charges is always unique.

Now we will analyze non-BPS black strings in model 2. For this case, the effective black string potential takes the form

$$V = \frac{1}{3}(\tilde{f}_1(p^1)^2 + 4x^4(p^2)^2 + \tilde{f}_2(p^3)^2 + \tilde{f}_3 p^1 p^2 + \tilde{f}_4 p^1 p^3 + \tilde{f}_5 p^2 p^3), \quad (6.17)$$

where we have introduced the functions

$$\begin{aligned} \tilde{f}_1 &= 36x^4 + 24x^3(2y+z) + 16x^2(y^2 + yz - 2z^2) - 12x(2yz^2 + z^3 + 1) - 4y + 9z^4 - 2z, \\ \tilde{f}_2 &= x^4 - 12x^3z + 90x^2z^2 - 324xz^3 + 6x + 729z^4 - 54z, \\ \tilde{f}_3 &= 4x(6x^3 + 2x^2(2y+z) - 3xz^2 - 2), \\ \tilde{f}_4 &= 2(6x^4 + x^3(4y-34z) - 3x^2z(8y-49z) + 2x(54yz^2 + 36z^3 - 1) - 81z^4 + 6z), \\ \tilde{f}_5 &= 4x^2(x^2 - 6xz + 27z^2). \end{aligned} \quad (6.18)$$

We will extremize this potential to obtain the equations of motion. We need to use the method of Lagrange multipliers to incorporate the constraint (5.22). We find

$$\begin{aligned} &(p^1)^2(-12x^4(2y+z) - 16x^3(y-z)(y+2z) + 18x^2z^2(2y+z) + 2x(2y-9z^4+z) - 3z^2) \\ &+ 2p^1x(x^3z(2p^2-17p^3) + x(2p^2+p^3)(2x^2(3x+y)-1) - 54p^3xyz^2 - 36p^3xz^3 + 81p^3z^4) \\ &+ 8(p^2)^2x^5 + p^3x^2(8p^2x^3 - 36p^2xz(x-3z) + p^3(2(x-3z)(x^2-6xz+27z^2)+3)) = 0, \\ &(p^3x - p^1z)(p^1(2x((x-9z)(6x^2+2x(2y+z)-3z^2)-1) + 9z) + 4p^2x^3(x-9z) \\ &+ p^3x(2(x-9z)(x^2-6xz+27z^2)+9)) = 0. \end{aligned} \quad (6.19)$$

To simplify these equations, we will use charge ratios defined as  $r = p^1/p^3$  and  $s = p^2/p^3$  and the inhomogeneous coordinates  $\tau = x/z$  and  $t = y/z$ . In terms of these variables the above equations read as

$$\begin{aligned} &r^2(4(2t^2+2t-7)\tau^3 + 8(2t+1)\tau^4 - 9(2t+1)\tau^2 - 9(4t+1)\tau + 27) \\ &- 2r\tau((8s+4)\tau^4 + (6s+3)\tau^2 - 9\tau(2s+6t+5) - 18\tau^3 + 81) \\ &- \tau^2(8(s^2+s+1)\tau^3 - 3\tau^2(12s-2t+5) + 27(4s+3)\tau - 135) = 0, \end{aligned} \quad (6.20)$$

$$\begin{aligned} &(r-\tau)(r(8\tau^4 + 4(t-22)\tau^3 - 27(2t+1)\tau^2 + 9\tau + 81) + \tau(4(s+5)\tau^3 \\ &- 3\tau^2(12s-6t+7) + 135\tau - 405)) = 0 \end{aligned} \quad (6.21)$$

We will now solve these equations to obtain black string configurations. It can easily be seen that  $\tau = r$ ,  $t = s$  solves these equations. This set of solutions corresponds to the BPS string. To obtain the non-BPS black string solutions we will first consider the inverse problem where we express the charge ratios  $r$  and  $s$  in terms of the inhomogeneous coordinates  $\tau$  and  $t$ . This can be easily obtained from the equations of motion. We find two independent solutions for non-BPS black strings:

$$r = \tau, \quad s = -\frac{1}{\tau^2}(2\tau^3 + \tau^2(t+1) - 3\tau + 9), \quad (6.22)$$

and

$$r = -\frac{\tau(56\tau^3 - (27 - 54t)\tau^2 + 405\tau - 1215)}{24\tau^4 + 4(6t - 65)\tau^3 - 9(30t + 13)\tau^2 + 27\tau + 243}, \quad (6.23)$$

$$s = -\frac{2\tau^2(4\tau^2 - 34\tau^3 + 27t^2 - 24) + t(64\tau^3 - 99\tau^2 + 405\tau - 1215) + 144\tau - 324}{24\tau^4 + 4(6t - 65)\tau^3 - 9(30t + 13)\tau^2 + 27\tau + 243}. \quad (6.24)$$

The first set of equations (6.22) can be easily solved for the scalar moduli to obtain

$$\tau = r, t = -\frac{1}{r^2}(2r^3 + r^2(s + 1) - 3r + 9). \quad (6.25)$$

Thus, for a given set of charges, we have a unique solution in this branch. The resulting solution will lie inside the Kähler cone if  $r > 3$  and  $s < -(2r^3 + r^2 - 3r + 9)/r^2$ .

We will now analyze the second branch of non-BPS solutions given in (6.23) and (6.24). First solve (6.23) for  $t$  to obtain

$$t = -\frac{r(24\tau^4 - 260\tau^3 - 117\tau^2 + 27\tau + 243) + \tau(56\tau^3 - 27\tau^2 + 405\tau - 1215)}{6\tau^2(r(4\tau - 45) + 9\tau)} \quad (6.26)$$

Substituting this expression for  $t$  in (6.24) and simplifying we obtain

$$2\tau^4(12r^2 + 4r(3s + 8) + 27s + 9) - r\tau^3(268r + 270s + 135) - 27(r - 15)r\tau^2 + 27(r - 45)r\tau + 243r^2 = 0. \quad (6.27)$$

This is a quartic equation in  $\tau$ . Thus we can express the exact analytic solutions for  $\tau$  in terms of the charge ratios  $r$  and  $s$ . However, before we consider the exact solutions, we will qualitatively analyze the relevant equations for this branch of solutions.

From (6.23) and (6.24) we find that the charge ratios  $r$  and  $s$  are expressed as rational functions of  $\tau$  and  $t$ . The denominators of these rational functions vanish when

$$24\tau^4 + 4(6t - 65)\tau^3 - 9(30t + 13)\tau^2 + 27\tau + 243 = 0. \quad (6.28)$$

This defines a singularity curve in the moduli space. To see this, solve the above equation for  $t$  to obtain

$$t = -\frac{24\tau^4 - 260\tau^3 - 117\tau^2 + 27\tau + 243}{6\tau^2(4\tau - 45)} \quad (6.29)$$

The numerator has a single zero at  $\tau = \tau_0 \simeq 11.2506$  in the  $\tau > 3$  region. The denominator vanishes at  $\tau = 45/4$ . The value of  $t$  in the above equation remains positive for  $45/4 < \tau < \tau_0$ . This gives rise to a line in the moduli space which starts at  $\tau = \tau_0$  when  $t = 0$  and asymptotes to  $\tau = 45/4$  line as  $t \rightarrow \infty$ . Points on this curve do not correspond to any extremal black string configuration. This singularity curve divides the moduli space into two regions, say region 1 and region 2. As we approach it from either of the regions the charge ratios diverge. Any point interior to either of the regions corresponds to a possible non-BPS black string configuration. The equations of

motion (6.23) and (6.24) guarantee the existence of such attractor configurations. In region 1, at the boundary point ( $\tau = 3, t = 0$ ) the charge ratios take values  $r = 141/215$  and  $s = -56/215$ . These are the minimum possible values for  $r$  and  $s$  in region 1. These values change from point to point and they diverge as we approach the singularity curve from the left. Similarly we can notice that, in region 2 the charge ratios take the maximum values  $r = -7/3$  and  $s = -1/3$  as  $\tau \rightarrow \infty$ . For any finite  $t$  these values decrease monotonically with  $\tau$  in this region and diverge as we go closer to the singularity curve from the right.

The above analysis indicates that these solutions are mutually exclusive to the first branch of solutions given in (6.25). We would like to investigate whether there exist multiple black string configurations for the second branch of solution. We first consider extremizing  $s$  in (6.24) as a function of  $\tau$  and  $t$ . Numerically solving the equations  $\partial s / \partial \tau = \partial s / \partial t = 0$  we find that they do not admit any solution inside the Kähler cone. We can further check if there exists an extremum in  $\tau$  for a fixed value of  $t$ . Setting  $\partial s / \partial \tau = 0$  for fixed  $t$ , we find

$$\begin{aligned} &108\tau^4 t^2 + 36\tau(6\tau^4 + \tau^3 + 45\tau^2 - 459\tau + 1458)t \\ &+ (112\tau^6 - 108\tau^5 + 3561\tau^4 - 27522\tau^3 \\ &+ 71685\tau^2 + 24786\tau - 10935) = 0. \end{aligned} \quad (6.30)$$

This is a quadratic equation in  $t$  with positive coefficients in the  $\tau > 3$  region. Thus, it does not admit any solution with  $t > 0$ . As a result,  $s$  does not admit an extremum in  $\tau$  for a

fixed  $t$  inside the Kähler cone. Hence there cannot be any multiple solution for a given set of charges in this model.

We will now consider the exact solution of the quartic (6.27) for a given value of  $r$  and  $s$ . Introducing the notation

$$\begin{aligned} d_0 &= 243r^2, d_1 = 27r(r-45), & d_2 &= -27r(r-15), \\ d_3 &= -r(268r+270s+135), & d_4 &= 2(12r^2+4r(3s+8)+27s+9), \end{aligned} \quad (6.31)$$

the Eq. (6.27) can be rewritten as

$$\sum_{k=0}^4 d_k \tau^k = 0.$$

Depending on the sign of the coefficients  $d_k$  this can admit zero, two or four real roots. As we have argued above, for a given choice of the charge ratios at most one of these real roots will lie inside the Kähler cone. Denoting the solutions as  $\tau_{1\pm}$  and  $\tau_{2\pm}$  we have

$$\begin{aligned} \tau_{1\pm} &= -\frac{1}{12d_4} \left( 3d_3 + \sqrt{3(9d_3^2 - 24d_2d_4 - 2\mathcal{X})} \pm \sqrt{6\mathcal{X} + \frac{18\sqrt{3}(d_3^3 - 4d_2d_3d_4 + 8d_1d_4^2)}{\sqrt{3(9d_3^2 - 24d_2d_4 - 2\mathcal{X})}}} \right), \\ \tau_{2\pm} &= -\frac{1}{12d_4} \left( 3d_3 - \sqrt{3(9d_3^2 - 24d_2d_4 - 2\mathcal{X})} \pm \sqrt{6\mathcal{X} + \frac{18\sqrt{3}(d_3^3 - 4d_2d_3d_4 + 8d_1d_4^2)}{\sqrt{3(9d_3^2 - 24d_2d_4 - 2\mathcal{X})}}} \right). \end{aligned}$$

Here, for easy reading we have introduced the notations

$$e_1 = d_2^2 - 3d_1d_3 + 12d_0d_4, \quad e_2 = 2d_2^3 - 9d_2(d_1d_3 + 8d_0d_4) + 27(d_0d_3^2 + d_1^2d_4),$$

in terms of which we define

$$e_3 = e_2 + \sqrt{e_2^2 - 4e_1^3} \quad \text{and} \quad \mathcal{X} = 3d_3^2 - 8d_2d_4 - 2^{2/3}e_3^{1/3}d_4 - 2^{4/3}e_3^{-1/3}e_1.$$

Though we obtained multiple black hole solutions in these three parameters THCY models, the black string solutions for a given set of magnetic charges are unique. While this might be true for the examples studied here this is not the case in general. To see this we will consider an explicit example of three parameter model admitting multiple black string solutions. The polytope ID associated with this specific THCY is 146. It has Hodge numbers  $h_{1,1} = 3, h_{2,1} = 81$  and Euler number  $\chi = -156$ . The resolved weight matrix for this manifold is

$$Q = \begin{pmatrix} 0 & 0 & 1 & 1 & 1 & 0 & 1 \\ 0 & 1 & 0 & 1 & 0 & 1 & 1 \\ 1 & 0 & 0 & 1 & 0 & 0 & 1 \end{pmatrix}. \quad (6.32)$$

The nonvanishing intersection numbers associated with the THCY  $\mathcal{M}$  are  $f = 1/2, g = 4/3, i = 4/3, j = 8$ . Thus, the volume of  $\mathcal{M}$  is given by

$$\mathcal{V} = 3xyz + 4xz^2 + 4yz^2 + 8z^3. \quad (6.33)$$

The corresponding Mori cone matrix is

$$\mathcal{M}^i_j = \begin{pmatrix} -1 & 0 & 1 & 0 & 1 & 0 & 0 \\ -1 & 1 & 0 & 0 & 0 & 1 & 0 \\ 1 & 0 & 0 & 1 & 0 & 0 & 1 \end{pmatrix}. \quad (6.34)$$

The divisor class  $\{D_i\}$  is obtained from the (1,1) homology basis of  $\mathcal{M}$  as  $D_1 = J_3 - J_1 - J_2, D_2 = J_2, D_3 = J_1D_4 = J_3, D_5 = J_1, D_6 = J_2, D_7 = J_3$ . From the expression for the Mori cone matrix, we find the Kähler cone matrix to be  $3 \times 3$  identity matrix. Thus the Kähler cone conditions are  $x > 0, y > 0, z > 0$  or, in terms of the inhomogeneous coordinates  $\tau > 0, t > 0$  and  $z > 0$ . Using  $\mathcal{V} = 1$  constraint we can show that the condition  $z > 0$  can be derived from  $\tau > 0, t > 0$  and need not be imposed separately.

We will study black string solutions in this model. The effective black string potential is given by

$$V = \frac{1}{3}((z(3p^1y + 4p^1z + 3p^2x + 4p^2z) + p^3x(3y + 8z) + 8p^3z(y + 3z))^2 - 2(p^2(3p^1z + 3p^3x + 8p^3z) + p^3(p^1(3y + 8z) + 4p^3(x + y + 6z))))). \quad (6.35)$$

The equations of motion are given by

$$\begin{aligned} & (3y + 4z)(-p^3(3p^1 + 4p^3) + (3p^3x + 3p^1z + 8p^3z)(8p^3z(y + 3z) + p^3x(3y + 8z) \\ & + z(3p^2x + 3p^1y + 4p^1z + 4p^2z))) + (3x + 4z)(p^3(3p^2 + 4p^3) - (3p^3y + 3p^2z + 8p^3z) \\ & (8p^3z(y + 3z) + p^3x(3y + 8z) + z(3p^2x + 3p^1y + 4p^1z + 4p^2z))) = 0, \\ & (8z(y + 3z) + x(3y + 8z))(p^3(3p^2 + 4p^3) - (3p^3y + 3p^2z + 8p^3z)(8p^3z(y + 3z) \\ & + p^3x(3y + 8z) + z(3p^2x + 3p^1y + 4p^1z + 4p^2z))) + z(3y + 4z)(-8p^3(p^2 + 3p^3) \\ & - p^1(3p^2 + 8p^3) + (8p^3(x + y + 6z) + p^2(3x + 8z) + p^1(3y + 8z))(8p^3z(y + 3z) \\ & + p^3x(3y + 8z) + z(3p^2x + 3p^1y + 4p^1z + 4p^2z))) = 0. \end{aligned} \quad (6.36)$$

We now express these equations in terms of the rescaled quantities to find

$$\begin{aligned} & (r(3t + 4) - 3s\tau - 4s + 4t - 4\tau)(r(3t + 4) + s(3\tau + 4) + 4(t + \tau + 4)) = 0, \\ & r^2(3t + 4)^2(3t + 8) + 8r(3t + 4)(-4s + 3t^2 + 18t + 16) \\ & - 4s^2(9\tau^2 + 42\tau + 40) - 32s(3\tau^2 - 3(t - 4)\tau + 20) - 27\tau^2t^3 - 72\tau t^3 \\ & - 108\tau^2t^2 - 360\tau t^2 + 160t^2 - 128\tau^2 - 144\tau^2t - 448\tau t + 640t - 512\tau = 0. \end{aligned} \quad (6.37)$$

It is not instructive to express the analytical expressions for  $\tau$ ,  $t$  in terms of  $r$ ,  $s$ . Instead, we will focus on the inverse problem and express the charge ratios as rational functions of the inhomogeneous coordinates. We find the BPS solution  $r = \tau$ ,  $s = t$  and three branches of non-BPS attractors. They are given by

$$r = \tau, s = -t - \frac{8(\tau + 2)}{3\tau + 4}, \quad (6.38)$$

$$r = -3\tau - \frac{8(t + 2)}{3t + 4}, \quad s = t, \quad (6.39)$$

$$\begin{aligned} r &= -\frac{3\tau^2(3t + 4)^2 + 32(3t^2 + 4t - 4) + 36\tau(3t^2 + 10t + 8)}{(3t + 4)(9\tau t + 12(\tau + t) - 40)}, \\ s &= -\frac{3t^2(3\tau + 4)^2 + 32(3\tau^2 + 4\tau - 4) + 36t(3\tau^2 + 10\tau + 8)}{(3\tau + 4)(9\tau t + 12(\tau + t) - 40)}. \end{aligned} \quad (6.40)$$

We can easily invert (6.38) and (6.39) to express the inhomogeneous coordinates in terms of  $r$ ,  $s$ . We find

$$\tau = r, t = -s - \frac{8(r + 2)}{3r + 4}, \quad (6.41)$$

$$\tau = -r - \frac{8(s + 2)}{3s + 4}, \quad t = s. \quad (6.42)$$

The first solution (6.41) lies within the Kähler cone for  $r > 0$  and  $s < -8(r + 2)/(3r + 4)$  where as the second solution (6.42) lies within the Kähler cone for  $s > 0$  and  $r < -8(s + 2)/(3s + 4)$ .

To invert (6.40), we will first do a shift and rescale the quantities as  $\tau = 4(\tilde{\tau} - 1)/3$ ,  $t = 4(\tilde{t} - 1)/3$ ,  $r = 4(\tilde{r} - 1)/3$  and  $s = 4(\tilde{s} - 1)/3$ . The equations take a simpler form in terms of these variables. We find

$$\begin{aligned} \tilde{r}\tilde{t}(2\tilde{t}\tilde{\tau} - 7) + 2\tilde{t}^2\tilde{\tau}^2 + 3\tilde{t}\tilde{\tau} - 3 &= 0, \\ \tilde{s}\tilde{t}(2\tilde{t}\tilde{\tau} - 7) + 2\tilde{t}^2\tilde{\tau}^2 + 3\tilde{t}\tilde{\tau} - 3 &= 0. \end{aligned} \quad (6.43)$$

Solving the above equations we find  $\tilde{\tau} = \tilde{t}\tilde{r}/\tilde{s}$  with

$$\begin{aligned}\tilde{t}_{1\pm} &= -\frac{1}{4} \left( \tilde{s} + \sqrt{\tilde{s}^2 + 4\tilde{g}} \pm 2\sqrt{\frac{\tilde{s}^2(\tilde{r}\tilde{s} - 34)}{2\tilde{r}\sqrt{\tilde{s}^2 + 4\tilde{g}}} + \frac{\tilde{r}\tilde{s}^2 - 2\tilde{g}\tilde{r} - 6\tilde{s}}{2\tilde{r}}} \right), \\ \tilde{t}_{2\pm} &= -\frac{1}{4} \left( \tilde{s} - \sqrt{\tilde{s}^2 + 4\tilde{g}} \pm 2\sqrt{\frac{\tilde{s}^2(\tilde{r}\tilde{s} - 34)}{2\tilde{r}\sqrt{\tilde{s}^2 + 4\tilde{g}}} + \frac{\tilde{r}\tilde{s}^2 - 2\tilde{g}\tilde{r} - 6\tilde{s}}{2\tilde{r}}} \right).\end{aligned}\quad (6.44)$$

where  $\tilde{g}$  is given by

$$\begin{aligned}\tilde{g} &= \frac{\tilde{s}}{23^{2/3}\tilde{r}} ((225(2\tilde{r}\tilde{s} + 1) + \tilde{f})^{1/3} \\ &+ (225(2\tilde{r}\tilde{s} + 1) - \tilde{f})^{1/3} - 23^{2/3}).\end{aligned}\quad (6.45)$$

In the above we have used the notation

$$\tilde{f} = \sqrt{6(13068 + 24489\tilde{r}\tilde{s} + 39924\tilde{r}^2\tilde{s}^2 - 1372\tilde{r}^3\tilde{s}^3)}.\quad (6.46)$$

The solution will remain inside the Kähler cone for  $\tilde{\tau} > 1, \tilde{t} > 1$ . Though there are four solutions in (6.44) for a given value of  $\tilde{r}, \tilde{s}$ , all of those do not satisfy the Kähler cone condition simultaneously. We need to find how many of those solutions lie inside the Kähler cone. This of course will depend on the values of  $\tilde{r}, \tilde{s}$ . Since  $\tilde{\tau} = \tilde{t}\tilde{r}/\tilde{s}$  we cannot have solutions satisfying the Kähler cone condition if  $\tilde{r}$  and  $\tilde{s}$  have opposite signs. In our notation, the Kähler cone condition for (6.41) is  $\tilde{r} > 1, \tilde{s} < -1 - 1/\tilde{r}$ , and for (6.42) it is  $\tilde{s} > 1, \tilde{r} < -1 - 1/\tilde{s}$ . Thus the three solutions (6.41), (6.42), and (6.44) are mutually exclusive. Let us now consider the case when  $\tilde{r}$  and  $\tilde{s}$  have the same sign. To understand this in detail let us eliminate  $\tau$  from the equations of motion described by (6.43) to obtain the following quartic in the variable  $\tilde{t}$

$$2\tilde{r}^2\tilde{t}^4 + 2\tilde{r}^2\tilde{s}\tilde{t}^3 + 3\tilde{r}\tilde{s}\tilde{t}^2 - 7\tilde{r}\tilde{s}^2\tilde{t} - 3\tilde{s}^2 = 0.\quad (6.47)$$

First consider the case when both  $\tilde{r}$  and  $\tilde{s}$  are positive. In the quartic (6.47) the coefficients change sign only once. Thus, according to Descartes rule of signs there is only one positive root for  $\tilde{t}$ . By suitable choice of the charge ratios we can make  $\tilde{t} > 1$  to obtain a unique non-BPS black string solution inside the Kähler cone. However, since the BPS solutions also exist for  $\tilde{r} > 1, \tilde{s} > 1$  region, these two solutions are not mutually exclusive from each other. Finally consider the case where both  $\tilde{r}$  and  $\tilde{s}$  are negative. For charge ratios valued in this range the coefficients in the quartic (6.47) change three times. Thus the equation can admit three positive roots for  $\tilde{t}$ . By suitable choice of the charge ratios it might be possible to have more than one non-BPS attractors existing inside the Kähler cone. This is indeed the case as a numerical analysis shows. Here we numerically solve the Eq. (6.47) for  $\tilde{t}$  upon setting  $\tilde{r} = -6n, \tilde{s} = -5n$  with  $n = 2, 3, \dots, 10$ . In each case there are three positive roots for  $\tilde{t}$  with two of them having values greater than 1. Since  $\tilde{\tau} = \tilde{t}\tilde{r}/\tilde{s} > \tilde{t}$  for these choices of charge ratios, we have multiple non-BPS black strings. In Fig. 7 we have presented the two black string solutions obtained for different values of  $n$ .

### A. Stability

We will now analyze stability of these non-BPS black strings. For this we need to compute the recombination

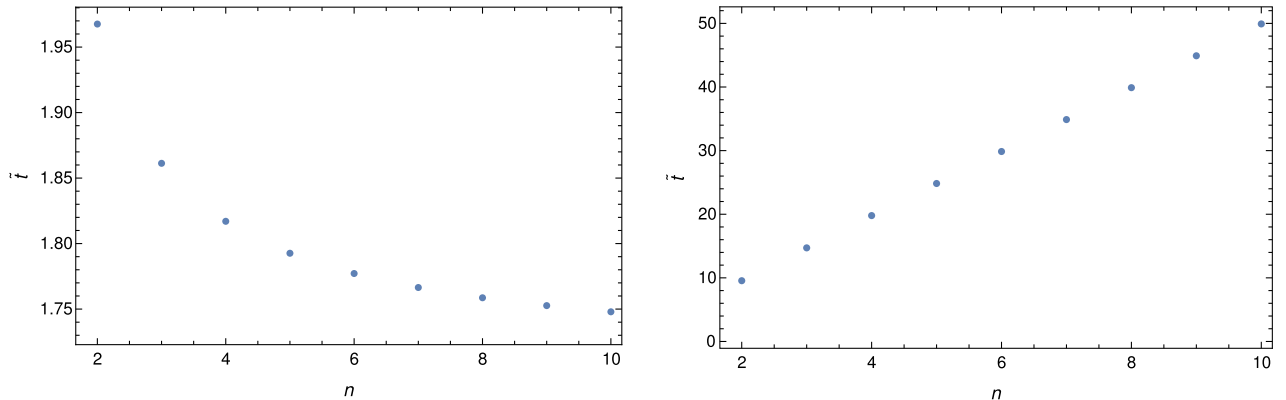


FIG. 7. Multiple non-BPS black strings in model 3 for  $\tilde{r} = -6n, \tilde{s} = -5n$  with  $n = 2, 3, \dots, 10$ . In the first case the value of  $\tilde{t}$  decreases with increasing  $n$  whereas in the second case it increases with  $n$ .



factor for the black string. The recombination factor is defined as the ratio of the volume of the nonholomorphic divisor on which the  $M5$  brane wraps to give rise to the non-BPS black string, to the volume of minimal piece-wise calibrated cycle in the same homology class as the non-holomorphic divisor under consideration. For double extremal black strings, the asymptotic volume of the non-holomorphic divisor is given by the square root of the effective black string potential at the attractor value. For a black string of charge  $p^I$ , the volume of the minimal piece-wise calibrated cycle is  $\sum_I |p^I| C_I$ , where  $C_I$  is the volume of the divisor  $J_I$ :

$$C_I = \int_{J_I} J \wedge J = C_{IJK} t^J t^K. \quad (6.48)$$

Denoting  $R$  as the recombination factor, we have

$$R = \frac{\sqrt{V_{\text{cr}}}}{\sum_I |p^I| C_I}. \quad (6.49)$$

For a three parameter model, the recombination factor is given as

$$R = \frac{\sqrt{V_{\text{cr}}}}{|p^1| C_1 + |p^2| C_2 + |p^3| C_3}, \quad (6.50)$$

where the volumes  $C_I$  are given in (3.5). We can substitute the expression for the black string solution in it to obtain the value of  $R$ . We will first compute the recombination factor for non-BPS black strings in model 1 before turning our discussion into the stability issues solutions in model 2. In the case of model 1, there are three branches of non-BPS solutions. Let us first consider the recombination factor for the first branch of solutions given in (6.14). In this case  $s > 0$  and  $r < 2-4s$ . We will consider the cases  $0 < r < 2-4s$  and  $r < 0$  separately. Substituting the explicit expressions for the solution (6.14) in (6.50) and simplifying, we find the recombination factor in the case  $s > 0$  and  $0 < r < 2-4s$  to have the form

$$R = 3(2s(s+1)(2-r-2s))^{1/3}. \quad (6.51)$$

In this case,  $R$  always remains greater than one if  $s > s_0$ , where  $s_0 \simeq 0.09$  is a root of the equation  $108(s^3 + s^2) = 1$  and the resulting black strings are all unstable. For  $0 < s < s_0$  the black strings are stable if  $\max\{0, -(108s^3 - 108s + 1)/54s(s+1)\} < r < 2-4s$  and unstable otherwise.

For  $s > 0$  and  $r < \min\{0, 2-4s\}$  the recombination factor becomes

$$R = \frac{3(2s(s+1))^{1/3}(2-r-2s)^{4/3}}{(2-3r-2s)}. \quad (6.52)$$

In this case  $R > 1$  for in the entire range of allowed values for  $r$  and  $s$ . Thus, in this case the black strings are all unstable.

For the second branch (6.15),  $r$  and  $s$  are valued in the range  $-1/2 < s < 0$ ,  $r > 2-4s$ . The recombination factor for this branch is given by

$$R = \frac{3(-2s)^{1/3}((s+1)(2s+r-2))^{4/3}}{(2s+1)(r(s+3)-2(s^2+3))}. \quad (6.53)$$

From the above expression we find that there is no stable attractor for  $-1/2 < s < -1/3$  irrespective of the values taken by  $r$ . For  $-1/3 < s < 0$ , the attractors become stable if  $2-4s < r < r_0$ , where the value of  $r_0$  is obtained by solving  $R = 1$  in (6.53) for  $r$  for a fixed value of  $s$ .

Finally we consider the third branch of solutions (6.16). In this case  $-1/2 < s < 0$  and  $r < 2$ . We will first consider the range  $-1/2 < s < 0$ ,  $0 < r < 2$ . In this case the recombination factor is

$$R = \frac{3(-2s)^{1/3}((s+1)(r+2s-2))^{4/3}}{(2s+1)(2s^2-rs+r+8s-2)}. \quad (6.54)$$

In this case the black strings are unstable for  $-1/2 < s < s_0$ , where  $s_0 \simeq -0.26$  is a root of  $108s^2(s+1)^4 - (s+3)^3(2s+1)^3 = 0$ . For  $s_0 < s < 0$  the black strings become unstable in the range  $0 < r < r_0$  and stable for  $r_0 < r < 2$ , where the value of  $r_0$  for a fixed  $s$  is determined by  $54s(s+1)^4(r+2s-2)^4 - (2s+1)^3(2s^2-rs+r+8s-2)^3 = 0$ .

Consider now the third branch of solutions (6.16) with  $-1/2 < s < 0$  and  $r < 0$ . In this case the recombination factor becomes

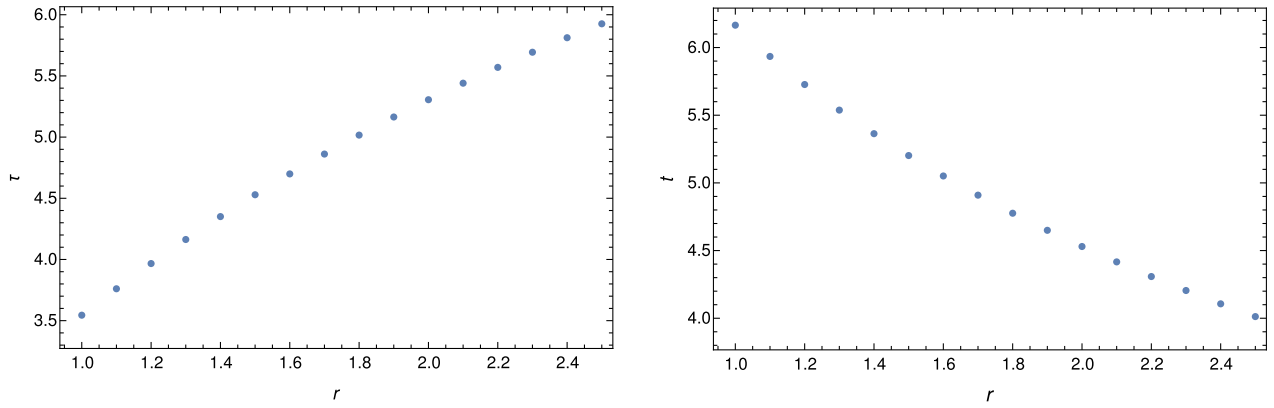
$$R = \frac{3(-2s)^{1/3}((s+1)(r+2s-2))^{4/3}}{(2s+1)(r(s+3)+2(s^2+4s-1))}. \quad (6.55)$$

In this case the attractors are unstable for  $-1/2 < s < s_0$  where  $s_0 \simeq -0.036$  is a root of the equation  $2048s(s+1)^5 + (s+3)^4(2s+1)^3 = 0$ . For  $s_0 < s < 0$  the attractors are stable for  $r_2 < r < r_1$  where  $r_{1,2}$  are obtained by solving  $R = 1$  in (6.55) for  $r$  for a fixed value of  $s$ .

Let us focus on the recombination factor for non-BPS black strings in model 2. We will first consider the solution (6.25). In this case, the recombination factor (6.50) takes the simple form

$$R = \frac{3r(2r^2 + 2rs + r - 3) + 27}{r(2r^2 + 6rs + r - 3) + 9}. \quad (6.56)$$

Recall that the solution (6.25) exists for  $r > 3$  and  $s < -(2r^3 + r^2 - 3r + 9)/r^2$ . For any given  $r$ , the recombination factor takes the minimum value  $R = 3/5$  when  $s$


 FIG. 8. Non-BPS black string solutions in region 1 with  $s = 3/2$  and  $1 \leq r \leq 5/2$ .

takes the maximum value  $s = -(2r^3 + r^2 - 3r + 9)/r^2$ . The value of  $R$  increases as  $s$  becomes more negative and approaches the value  $R = 1$  as  $s \rightarrow -\infty$ . Thus  $R < 1$  for all the black strings in this branch of solutions and hence they are all stable.

We will now consider the recombination factor for the second branch of solutions described by (6.26) and (6.27). The resulting expression is complicated and it is not possible to extract any insight from it. In what follows, we will numerically solve the equations of motion for various choices of the charge ratios and substitute the resulting solutions to obtain the values of the respective recombination factors. We first consider a fixed value for  $s$ , ( $s = 3/2$ ) and vary  $r$  in the range  $1 \leq r \leq 5/2$ . This leads solutions in region 1. We notice the value of  $\tau$  increases monotonically with the increase of  $r$  while the value of  $t$  decreases. The plot for the inhomogeneous coordinates  $\tau$  and  $t$  are given in Fig. 8. Further we consider the value  $s = -3/2$  and vary  $r$  in the range  $-24 \leq r \leq -3$  to obtain solutions in region 2. In this case, both the inhomogeneous coordinates increase with  $r$ . The results are given in the Fig. 9.

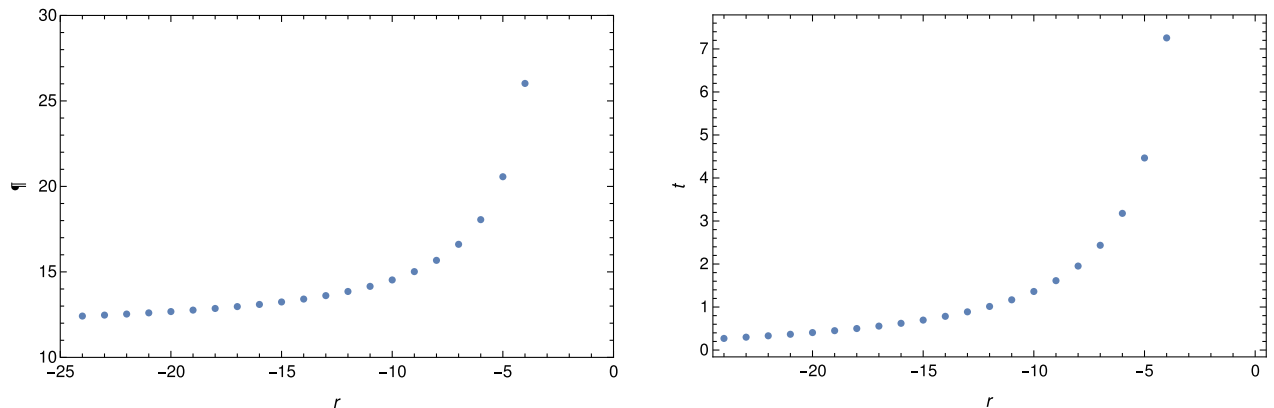
The recombination factors for solutions in both the regions are depicted in Fig. 10. In region 1 the value of

recombination factor increases with  $r$  whereas in region 2 it decreases. We observe that the value of  $R$  remains less than one in both the regions and it tends to saturate to 1 as we approach the singularity curve. Thus the corresponding black strings in the interior of regions 1 and 2 are all stable. We have considered a wide range of charges and numerically evaluated the recombination factor for all these choices. We could not find any case with  $R > 1$ . This suggests that the black strings corresponding to the second branch of solutions are also stable.

Finally we turn our attention to the stability of non-BPS black strings in model 3. We will first consider the solutions given in (6.41) and (6.42). The recombination factors for these two cases are given respectively as

$$R = \frac{3(3rs + 4r + 4s + 8)}{9rs + 4r + 12s + 8} \quad \text{and} \quad R = \frac{3(3rs + 4r + 4s + 8)}{9rs + 12r + 4s + 8}. \quad (6.57)$$

In both these cases the value of  $R$  remains less than 1 in the allowed range of the charge ratios. We can check this easily by expressing  $R$  in terms of the inhomogeneous coordinates. In both the cases,  $R$  has a minimum value of  $3/5$  and it increases monotonically with  $\tau$  and  $t$  and approaches the


 FIG. 9. Non-BPS black string solutions in region 2 with  $s = -3/2$  and  $-24 \leq r \leq -3$ .

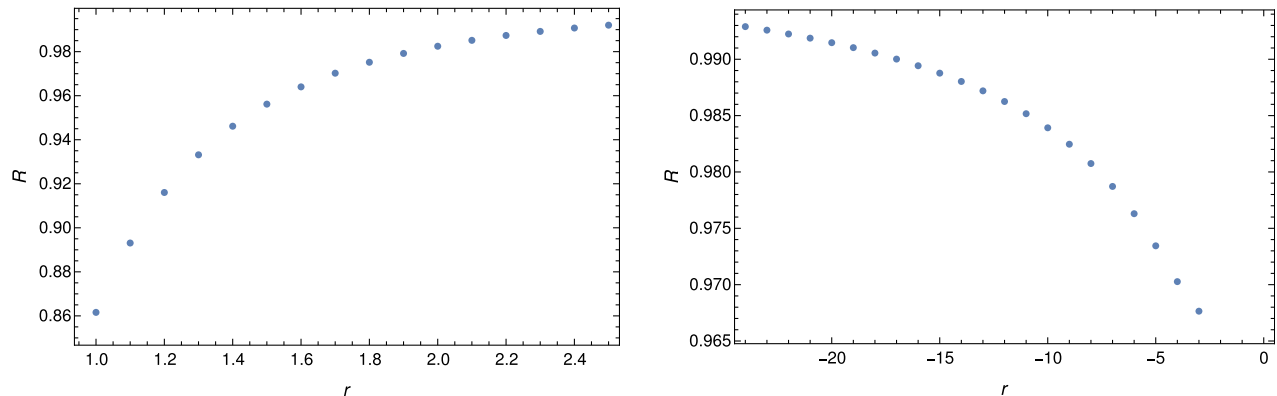


FIG. 10. Recombination factors corresponding to the solutions in both the regions. The figure in the left corresponds to recombination factors in region 1 and the one in the right corresponds to recombination factors in region 2.

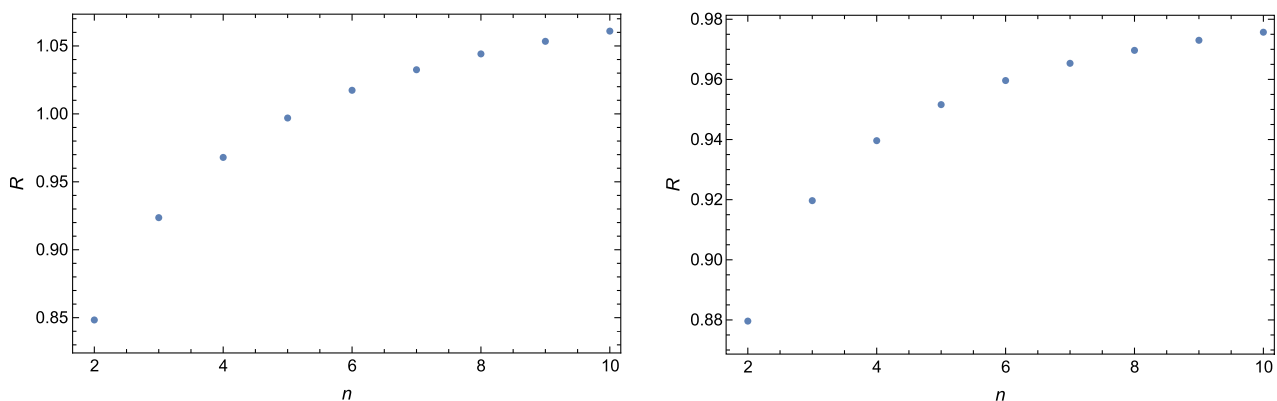


FIG. 11. Recombination factors for the multiple solutions corresponding to Fig. 7.

maximum value  $R = 1$  when either of these coordinates becomes infinite. Thus the corresponding black strings are all stable. For the solutions (6.47) we have obtained the recombination factors numerically. As we can see from Fig. 11, depending the value of  $n$  the recombination factor becomes larger or smaller than one. Thus, in this case we have both stable as well as unstable non-BPS black string solutions.

## VII. CONCLUSION

In this paper we have studied BPS as well as non-BPS black branes in five dimensional supergravity theories arising from the compactification of M-theory on three parameter Calabi-Yau manifolds. We considered two explicit examples of toric Calabi-Yau manifolds with  $h_{1,1} = 3$  and obtained all BPS and non-BPS black hole configurations in them. For the first model, the resulting BPS solutions were unique for a given set of charges. However, for model 2, we found multiple BPS black hole solutions when their charges are valued in a particular range. The non-BPS black holes for model 1 admit three independent solutions. However, they are mutually exclusive

from each other and for a given set of black hole charges, there is a unique solution. For the non-BPS black holes in model 2, the moduli space admits two singularity curves. Points on the singularity curves do not correspond to any black hole solution. They divide the moduli space into three regions. Any point in a given region corresponds to a possible non-BPS attractor for some suitable choice of black hole charges. As we change the charges the points move within a given region. But they never cross the singularity curves for finite values of black hole charges. This model also admits multiple non-BPS black holes. We considered the stability of doubly extremal non-BPS black hole configurations in these models and found that the black holes become stable for a range of charges. This is in contrast to the examples studied in [10] and the two parameter models in [14] where the non-BPS black hole configurations were all unstable. Moreover none of the models considered in [10,14] admitted multiple black hole solutions.

Subsequently we have studied non-BPS black string solutions in these models. Once again we found three independent non-BPS solutions in model 1. They were all mutually exclusive and hence we have unique non-BPS

black string solution for a given set of charges. Model 2 admitted two branches of solutions. The second branch of solutions admitted a singularity curve which divided the moduli space into two regions. Points on the singularity curve did not correspond to non-BPS attractors for any choice of the black string charges. Further, we found that for a given set of charges the resulting black string solution was always unique. To demonstrate the existence of multiple non-BPS black string solutions we considered one more three parameter Calabi-Yau model. We obtained all black string solutions in this model and observed that it admits multiple non-BPS solutions in a given range of black string charges. We have also analyzed the stability of the doubly extremal black string configurations corresponding to all the attractor values we have obtained. It is interesting to observe

so much rich structure for attractor configurations in three parameter Calabi-Yau models. It would be worth investigating the behavior of both BPS as well as non-BPS multiple attractor configurations in more detail. In four dimensions, incorporating  $D6$  branes gives a rich structure both in the BPS as well as non-BPS sector [26–29]. Extending the analysis of [15] to incorporate the  $D6$  branes and relating them with the solutions studied here using the 4D–5D correspondence [30] is another interesting aspect that needs to be explored. We hope to analyze these issues in future.

## ACKNOWLEDGMENTS

We would like to thank Alessio Marrani for collaboration in [14] as well as for useful correspondences.

- 
- [1] M. R. Douglas, *J. High Energy Phys.* **05** (2003) 046.
  - [2] C. Vafa, [arXiv:hep-th/0509212](https://arxiv.org/abs/hep-th/0509212).
  - [3] H. Ooguri and C. Vafa, *Nucl. Phys.* **B766**, 21 (2007).
  - [4] N. Arkani-Hamed, L. Motl, A. Nicolis, and C. Vafa, *J. High Energy Phys.* **06** (2007) 060.
  - [5] S. Ferrara, R. Kallosh, and A. Strominger, *Phys. Rev. D* **52**, R5412 (1995).
  - [6] S. Ferrara and R. Kallosh, *Phys. Rev. D* **54**, 1514 (1996).
  - [7] S. Ferrara and R. Kallosh, *Phys. Rev. D* **54**, 1525 (1996).
  - [8] S. Ferrara, G. W. Gibbons, and R. Kallosh, *Nucl. Phys.* **B500**, 75 (1997).
  - [9] K. Goldstein, N. Iizuka, R. P. Jena, and S. P. Trivedi, *Phys. Rev. D* **72**, 124021 (2005).
  - [10] C. Long, A. Sheshmani, C. Vafa, and S. T. Yau, *Commun. Math. Phys.* **399**, 1991 (2023).
  - [11] M. Gunaydin, G. Sierra, and P. K. Townsend, *Nucl. Phys.* **B253**, 573 (1985).
  - [12] A. C. Cadavid, A. Ceresole, R. D’Auria, and S. Ferrara, *Phys. Lett. B* **357**, 76 (1995).
  - [13] S. Ferrara, R. R. Khuri, and R. Minasian, *Phys. Lett. B* **375**, 81 (1996).
  - [14] A. Marrani, A. Mishra, and P. K. Tripathy, *J. High Energy Phys.* **06** (2022) 163.
  - [15] J. Aspmann and J. Manschot, [arXiv:2212.10645](https://arxiv.org/abs/2212.10645).
  - [16] R. Kallosh, A. D. Linde, and M. Shmakova, *J. High Energy Phys.* **11** (1999) 010.
  - [17] M. Gunaydin, G. Sierra, and P. K. Townsend, *Nucl. Phys.* **B242**, 244 (1984).
  - [18] A. S. Chou, R. Kallosh, J. Rahmfeld, S. J. Rey, M. Shmakova, and W. K. Wong, *Nucl. Phys.* **B508**, 147 (1997).
  - [19] S. Ferrara and M. Gunaydin, *Nucl. Phys.* **B759**, 1 (2006).
  - [20] B. L. Cerchiai, S. Ferrara, A. Marrani, and B. Zumino, *Phys. Rev. D* **82**, 085010 (2010).
  - [21] M. Kreuzer and H. Skarke, *Adv. Theor. Math. Phys.* **4**, 1209 (2000).
  - [22] R. Altman, J. Gray, Y. H. He, V. Jejjala, and B. D. Nelson, *J. High Energy Phys.* **02** (2015) 158.
  - [23] R. Altman, Y. H. He, V. Jejjala, and B. D. Nelson, *Phys. Rev. D* **97**, 046003 (2018).
  - [24] R. Altman, J. Carifio, X. Gao, and B. D. Nelson, *J. High Energy Phys.* **03** (2022) 087.
  - [25] <http://www.rossealtman.com/toriccy/index.html>.
  - [26] P. K. Tripathy and S. P. Trivedi, *J. High Energy Phys.* **03** (2006) 022.
  - [27] T. Mandal and P. K. Tripathy, *Phys. Lett. B* **749**, 221 (2015).
  - [28] A. Marrani, P. K. Tripathy, and T. Mandal, *Int. J. Mod. Phys. A* **32**, 1750114 (2017).
  - [29] P. K. Tripathy, *Phys. Lett. B* **770**, 182 (2017).
  - [30] A. Ceresole, S. Ferrara, and A. Marrani, *Classical Quantum Gravity* **24**, 5651 (2007).